Article

Current Biology

Flexible encoding of objects and space in single cells of the dentate gyrus

Graphical abstract

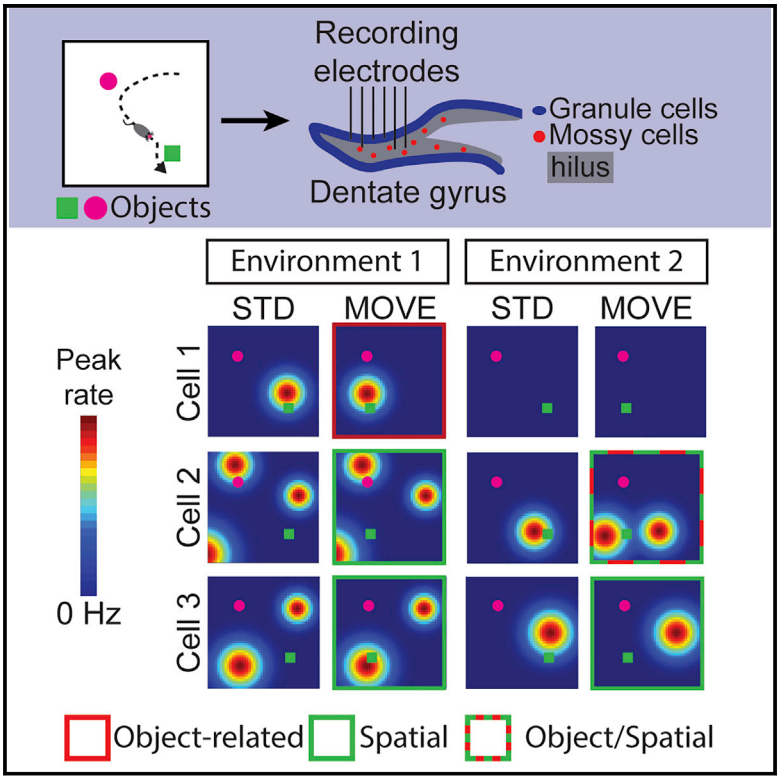

Highlights

- Object addition/manipulation alters the spatial firing of dentate gyrus cells
- Diverse object-related responses were observed, including landmark vector cells
- Object-related activity was evaluated separately in granule and mossy cells
- Object-related responses are not fixed within single cells or a dedicated population

Authors

Douglas GoodSmith, Sang Hoon Kim, Vyash Puliyadi, Guo-li Ming, Hongjun Song, James J. Knierim, Kimberly M. Christian

Correspondence

shongjun@pennmedicine.upenn.edu (H.S.),
jknierim@jhu.edu (J.J.K.),
kchristi@pennmedicine.upenn.edu (K.M.C.)

In brief

GoodSmith et al. report diverse responses of individual place fields of dentate gyrus (DG) cells to object manipulation. Unique groups of cells have object-related activity following global remapping between environments, suggesting that DG cells flexibly encode small nonspatial changes while maintaining a stable spatial map of the environment.

GoodSmith et al., 2022, Current Biology *32*, 1–14
March 14, 2022
https://doi.org/10.1016/j.cub.2022.01.023

CellPress

Please cite this article in press as: GoodSmith et al., Flexible encoding of objects and space in single cells of the dentate gyrus, Current Biology (2022), https://doi.org/10.1016/j.cub.2022.01.023

Current Biology

CellPress

Article

Flexible encoding of objects and space in single cells of the dentate gyrus

Douglas GoodSmith,[1,7,8,10,11] Sang Hoon Kim,[1,11] Vyash Puliyadi,[6,7] Guo-li Ming,[1,2,3,4] Hongjun Song,[1,2,3,5,*] James J. Knierim,[7,8,9,*] and Kimberly M. Christian[1,12,*]

[1]Department of Neuroscience and Mahoney Institute for Neurosciences, Perelman School of Medicine, University of Pennsylvania, 3400 Civic Center Boulevard, Philadelphia, PA 19104, USA
[2]Department of Cell and Developmental Biology, Perelman School of Medicine, University of Pennsylvania, 3400 Civic Center Boulevard, Philadelphia, PA 19104, USA
[3]Institute for Regenerative Medicine, Perelman School of Medicine, University of Pennsylvania, 3400 Civic Center Boulevard, Philadelphia, PA 19104, USA
[4]Department of Psychiatry, Perelman School of Medicine, University of Pennsylvania, 3400 Civic Center Boulevard, Philadelphia, PA 19104, USA
[5]The Epigenetics Institute, Perelman School of Medicine, University of Pennsylvania, 3400 Civic Center Boulevard, Philadelphia, PA 19104, USA
[6]Department of Psychological and Brain Sciences, Johns Hopkins University, 3400 N Charles Street, Baltimore, MD 21218, USA
[7]Zanvyl Krieger Mind/Brain Institute, Johns Hopkins University, 3400 N Charles Street, Baltimore, MD 21218, USA
[8]The Solomon H. Snyder Department of Neuroscience, Johns Hopkins University School of Medicine, 733 N Broadway, Baltimore, MD 21205, USA
[9]Kavli Neuroscience Discovery Institute, Johns Hopkins University School of Medicine, 733 N Broadway, Baltimore, MD 21205, USA
[10]Department of Neurobiology and Neuroscience Institute, University of Chicago, 5801 S Ellis Avenue, Chicago, IL 60637, USA
[11]These authors contributed equally
[12]Lead contact
*Correspondence: shongjun@pennmedicine.upenn.edu (H.S.), jknierim@jhu.edu (J.J.K.), kchristi@pennmedicine.upenn.edu (K.M.C.)
https://doi.org/10.1016/j.cub.2022.01.023

SUMMARY

The hippocampus is involved in the formation of memories that require associations among stimuli to construct representations of space and the items and events within that space. Neurons in the dentate gyrus (DG), an initial input region of the hippocampus, have robust spatial tuning, but it is unclear how nonspatial information may be integrated with spatial activity in this region. We recorded from the DG of 21 adult mice as they foraged for food in an environment that contained discrete objects. We found DG cells with multiple firing fields at a fixed distance and direction from objects (landmark vector cells) and cells that exhibited localized changes in spatial firing when objects in the environment were manipulated. By classifying recorded DG cells into putative dentate granule cells and mossy cells, we examined how the addition or displacement of objects affected the spatial firing of these DG cell types. Object-related activity was detected in a significant proportion of mossy cells. Although few granule cells with responses to object manipulations were recorded, likely because of the sparse nature of granule cell firing, there was generally no significant difference in the proportion of granule cells and mossy cells with object responses. When mice explored a second environment with the same objects, DG spatial maps completely reorganized, and a different subset of cells responded to object manipulations. Together, these data reveal the capacity of DG cells to detect small changes in the environment while preserving a stable spatial representation of the overall context.

INTRODUCTION

A hallmark feature of the hippocampus in rodents is the spatially tuned activity of its principal neurons. Place cells in the hippocampus fire whenever an animal passes through a specific location within an environment, and a place cell's activity within its place field can be modulated by nonspatial events and information.[1–9] An internal "cognitive map," formed by embedding nonspatial and object-related information onto a stable spatial framework, has been theorized to promote spatial navigation in animals and episodic memory in humans.[10–13] Most studies on the integration of nonspatial and spatial information have focused on CA1, but the dentate gyrus (DG) may be crucial for this function because of its position within the hippocampal circuit. The DG receives inputs from both the medial and lateral portions of the entorhinal cortex (MEC and LEC, respectively), and distinct patterns of spatial and nonspatial information have been reported in both MEC and LEC.[14–17] How single DG cells may integrate this information to support the formation of a cohesive neural representation of an experience is unclear.

The DG contains two excitatory cell types: granule cells in the granule cell layer and mossy cells in the hilus.[18] Although most

Please cite this article in press as: GoodSmith et al., Flexible encoding of objects and space in single cells of the dentate gyrus, Current Biology (2022), https://doi.org/10.1016/j.cub.2022.01.023

theories of DG function focus on the more numerous granule cells, mossy cells can broadly regulate granule cell activity directly and via DG interneurons.[19] Furthermore, the DG circuit contains a small population of excitable, immature adult-born granule cells (abGCs),[20] as well as multiple types of interneurons. As a result, DG function relies on the coordination and communication of multiple cell types within the DG circuit.[21–24] In behavioral studies, dorsal DG lesions do not affect the ability of an animal to discriminate among different objects, but they can impair learning of complex object-place configurations[25,26] or odor-context associations.[27] Similarly, targeted manipulation of mossy cell activity can affect object-related behaviors, with optogenetic[22] and chemogenetic[28] manipulations impacting either object-place learning or novel object recognition. Together, these results suggest an important role for the DG in the processing of object information and indicate that the DG may be essential for the conjunctive encoding of spatial and nonspatial signals from MEC and LEC.[29–31]

Although behavioral results support conjunctive encoding in the DG, it is unclear whether spatial and nonspatial information is integrated at the circuit level among different neuronal subpopulations or within single neurons. Determining the capacity of individual cells and specific cell types to exhibit firing patterns that are modulated by space, objects, or both is needed to understand how information about complex environments is represented in the two excitatory populations of the DG. In head-fixed mice, the addition of tactile cues to a treadmill induced or reorganized some granule cell and mossy cell firing fields and revealed differences between the cell types in the timing and duration of cue-modulated firing during learning.[32–34] Given the well-established ability of the hippocampus to generate highly stereotyped sequential representations of distance and time in linear tracks and treadmills, it can be difficult to disentangle neural responses to spatial information and tactile cues that are repeatedly experienced by the animal in a particular order. Therefore, it is critical to record from freely moving animals in an environment in which objects can be approached from multiple directions in a 2D coordinate frame to determine how spatial and nonspatial information is represented when not constrained by sequential presentations of stimuli and path-invariant sampling of space.

Technical challenges have limited the *in vivo* study of activity in identified DG cell types. In this study, we used a machine learning approach to classify granule cells and mossy cells recorded in the dorsal DG as mice foraged for food in environments with discrete objects that were manipulated in alternating sessions. Although most spatially modulated DG granule cells and mossy cells maintained a stable spatial representation of the environment, diverse object-related activity was also observed. Object responses were detected in a significant number of mossy cells, but not granule cells. However, there was generally no significant difference in the proportion of cells with object-related activity between DG cell types, suggesting that the low number of detected granule cell responses may have been due to the extremely sparse firing of these cells. Place field activity of both populations reorganized between environments (global remapping), and object-related activity was observed in different ensembles of DG cells in each environment, indicating that there is not a dedicated subpopulation of DG cells that respond to objects. Instead, these results suggest flexibility within the DG, in which many cells have the capacity to detect changes in object number and location and can be differentially responsive to local changes in the environment in a context-dependent manner.

RESULTS

Recording from classified DG cell types

Recording sessions with two objects in standard (STD) locations were alternated with manipulation (MAN) sessions, in which one object was moved (MOVE) or a third object was added (ADD) (Figures 1A–1C). Consistent with behavioral studies,[28,35,36] mice spent significantly more time within 5 cm of the manipulated object than the unmanipulated object (manipulated object: median 13, interquartile range [IQR] 7–19 s; unmanipulated object: median 8, IQR 4–14 s; signed-rank test $z = 3.22$, $p = 0.002$). We focused our primary analysis on excitatory cells, and 75 cells were excluded from analysis as putative interneurons (Figure S1). Of 366 well-isolated putative excitatory cells recorded in a sleep session from the hilus and granule cell layer (Figure 1D), 178 (49%) did not have a significant place field in any recording session and fired very few spikes, if any, which precluded analysis of object-related influences on spatial firing. The remaining 188 cells (51%) had at least one place field in at least one session, and these were the cells that could be quantitatively analyzed in the present study.

Mossy cells are much more active than granule cells, and a single mossy cell can be recorded on electrodes located up to 300 μm apart.[37–40] For this reason, it is difficult to infer cell identity based on the recording site alone. In previous work, we showed how machine learning techniques could be used to resolve the activity of these distinct DG cell types in rats.[23,37] In the present study, we utilized similar methods and generated a random forests classifier (Figure 2A) to assign putative cell types to cells recorded in the mouse DG based on their firing properties in a post-behavior rest/sleep session (STAR Methods; Figure 2B). Training data for this classifier were obtained from mouse DG cells recorded in a separate foraging task (recorded in the same mice but on different recording days; STAR Methods; Figure 2A). The classifier had an estimated error rate of ~5% (out-of-bag error; STAR Methods; Figure S2), suggesting reliable discrimination between cell types. Importantly, the classifier identified DG cell types on object recording days using firing properties recorded in the post-behavior sleep session only.

Of the 366 DG cells, there were 172 classified mossy cells and 194 classified granule cells; 83% of cells without place fields (147/178) were classified as granule cells, and 75% of cells with fields (141/188) were classified as mossy cells. Classified granule cells had fewer place fields (granule cells median 1, IQR 1–2; mossy cells median 2, IQR 1–2; rank-sum test $z = 3.75$, $p = 1.78 \times 10^{-4}$), lower mean firing rates (granule cells median 0.49 Hz, IQR 0.22–0.99; mossy cells median 0.83 Hz, IQR 0.46–1.39; rank-sum test $z = 5.52$, $p = 3.31 \times 10^{-8}$), and lower peak firing rates (granule cells median 7.38 Hz, IQR 3.15–14.00; mossy cells median 9.89 Hz, IQR 6.14–15.92; rank-sum test $z = 3.98$, $p = 6.93 \times 10^{-5}$) in behavior sessions than classified mossy cells. These results replicate recently reported

Please cite this article in press as: GoodSmith et al., Flexible encoding of objects and space in single cells of the dentate gyrus, Current Biology (2022), https://doi.org/10.1016/j.cub.2022.01.023

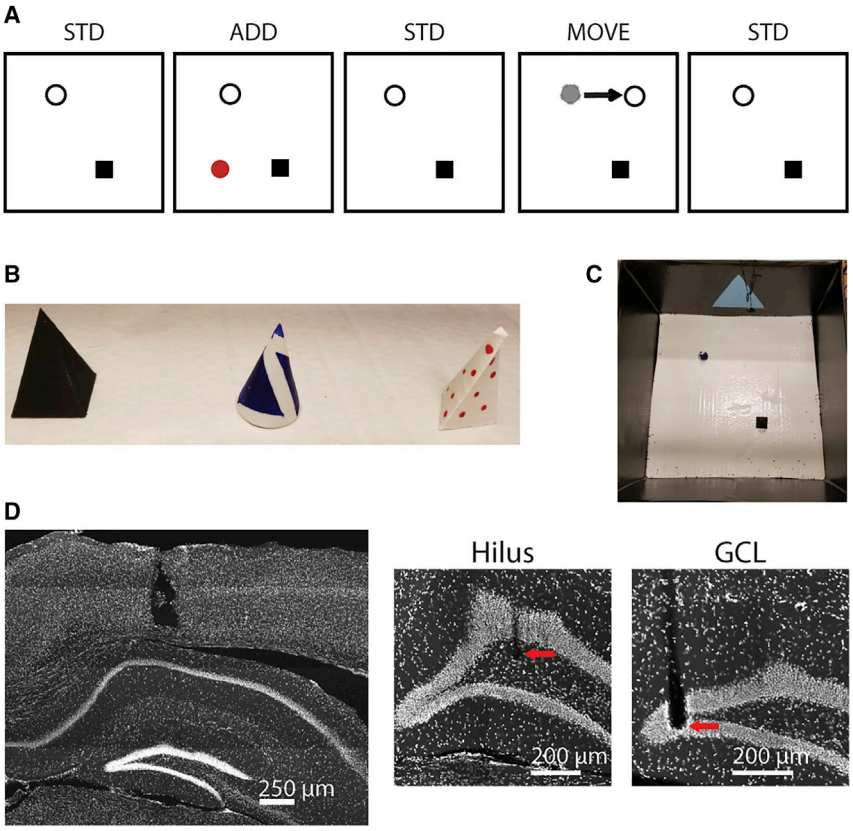

Figure 1. Behavioral task and DG recordings
(A) Schematic of example recording day. Standard (STD) sessions in which two objects in standard locations were alternated with manipulation (MAN) sessions, in which a third object was added (ADD) or one object was moved (MOVE).
(B) Picture of objects used; the two objects on the left are the STD objects.
(C) Picture of the environment with objects in the STD configuration.
(D) Image of the hippocampus (left) and higher magnification images of tetrode tracks terminating in the hilus and granule cell layer (GCL).

differences in firing properties between identified granule cells and mossy cells,[37,38,41,43] indicating that the classifier was able to distinguish DG cell types. Finally, although a recent study reported differences in the effects of mossy cell inhibition in male versus female mice,[28] we did not observe any significant differences in activity or behavior between male and female mice (Table S1).

Population activity and place field comparisons

We first measured the effect of object manipulation on overall DG activity levels by comparing the firing rates and place field properties of DG cells in STD and MAN sessions. There was no significant difference in the median values of the mean or peak firing rates between the STD and MAN sessions for granule cells or mossy cells meeting inclusion criteria (Table S2 for statistics; Figures 3A and 3B). There was also no significant difference in the firing rates of granule cells or mossy cells near (within 10 pixels, ~14 cm) and away (>10 pixels) from all objects (Table S2 for statistics; Figure 3C). Thus, at a population level, neither cell type overrepresented locations near objects with an increased firing rate. Object manipulation did not generally cause the formation or enlargement of place fields; place fields were detected in a similar proportion of STD and MAN sessions, and the number and average size of place fields in spatially modulated cells did not differ in STD versus MAN sessions (Table S2 for statistics; Figures 3D and 3E). No significant differences in these properties were observed when restricting our analysis to ADD sessions (Table S2). Together, these results demonstrate that the addition and manipulation of objects within the environment did not significantly and coherently alter firing rates or place field size/number in either the granule cell or mossy cell population.

Presence of landmark vector cells

Although we did not detect any significant population differences in firing rate or place field size/number, visual inspection of the rate maps revealed that many DG cells appeared to have firing related to the presence of objects within the environment. Some of these cells fired at a fixed vector relationship (same distance and direction) to objects/landmarks within the environment, consistent with responses of previously described landmark vector (LV) cells.[4,5,17] To identify LV responses in a single recording session, it is necessary to analyze cells with at least two firing fields to establish the vector relationship across objects. Putative LV cells were identified based on the minimum pairwise difference between vectors connecting objects to place field centers[4] (STAR Methods; Figure 4A).

LV responses were detected in 37 mossy cells and 10 granule cells (Figures 4B and 4C). LV responses were observed in more than one session (Figure 4C) for 8/37 mossy cells and 3/10 granule cells. Because mossy cells were more likely than granule cells to have the multiple place fields required to detect a LV response in a session, we compared the proportion of LV responses detected in sessions with at least two fields and found no significant difference between cell types (granule cells: 13/58; mossy cells: 50/273; $\chi_{(1)}^2 = 0.52$, $p = 0.47$). The magnitude and variability of the detected LV responses was also similar between the cell types because there was no significant difference in the distribution of minimum vector differences between granule cells and mossy cells (rank-sum test $z = 0.21$, $p = 0.83$; Figures 4D and 4E). The number of LV responses was significantly greater than the number obtained by randomizing place field locations[4] (STAR Methods) for mossy cells ($p < 0.01$), but granule cells only showed a statistical trend in that direction ($p = 0.06$) (Figure 4F), even when a stricter threshold was used for LV detection (Figure S3). In summary, a significant number of LV responses were detected in the DG. Importantly, there was no significant difference between cell types in the minimum

Please cite this article in press as: GoodSmith et al., Flexible encoding of objects and space in single cells of the dentate gyrus, Current Biology (2022), https://doi.org/10.1016/j.cub.2022.01.023

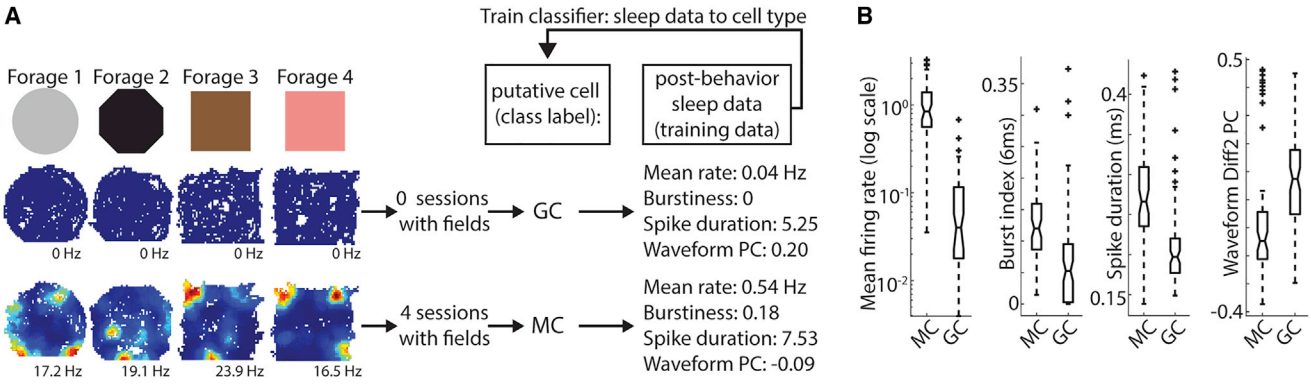

Figure 2. Classification of DG cell types

(A) Cells recorded in a foraging task (without objects) were used to train a classifier to separate putative granule cells and mossy cells. DG cells were recorded as animals foraged for food in four distinct environments. Blue pixels in rate maps reflect areas with no spikes, whereas red pixels correspond to the peak firing rate (below each map). Based on previous reports of DG place fields,[37,38,41,42] most granule cells have no place fields in any environment and most mossy cells have place fields in most environments. We therefore considered any cell with no fields in any session as a putative granule cell and any cell with fields in 3 or more sessions as a putative mossy cell. After these putative cell type labels were assigned, the properties of these cells in a post-behavior sleep session were identified. These firing features were used as the training data, and a random forests classifier was trained to classify the training data to the putative cell-type labels.

(B) Features used for classification. As classification features are correlated with cell type, these plots are presented for display purposes only and statistical comparisons were not performed. Boxplots indicate the values for putative granule cells (GCs) and mossy cells (MCs) in our training data. The dashed line indicates the range of data (outliers marked +), horizontal lines indicate the median, 25th percentile, and 75th percentile, and notches indicate the 95% CI of the median. From left to right: mean firing rate, burst index, spike duration, and first principal component of the second derivative of the waveform.

See also Figures S1 and S2.

vector difference distribution or the proportion of detected LV responses, suggesting that any DG cell with two or more fields had a similar probability of having a detected LV response with similar characteristics

Diverse DG cell responses to object manipulation

Additional object-related firing changes following object manipulations could be divided into at least six different response categories (Figure 5). "Moved field" responses (cells with firing fields located near an object both before and after that object was moved) frequently appeared in our recordings (moved field; Figure 5B). These fields often maintained their vector relationship with the moved object, similar to LV responses. Other times, however, a field maintained its distance to the moved object but rotated to a different angle relative to the object (rotation; Figure 5C). We also observed "trace cells," which fired at the location where a moved object had previously been[4,44,45] (trace; Figure 5D). Trace responses do not reflect the current relationship between objects and the environment but instead reflect some "memory" of a previous object configuration. Other cells had place fields that appeared at the location of a new or moved object (appear; Figure 5E) or disappeared when an object was placed near the field location (disappear; Figure 5F). Finally, "capture" responses occurred when an existing place field moved closer to a new or moved object (capture; Figure 5G).

Object-related firing was only observed in a subset of DG cells; most cells and individual place fields displayed stable spatial firing patterns (Figure S4), as expected from hippocampal place fields. Intriguingly, place fields of the same cell were often differentially affected by object manipulations, which suggests that DG cells are not specialized for either spatial or object-related firing. Individual fields of a DG cell can exhibit varied responses to objects ranging from a stable spatial field with no object-related modulation (Figure S4) to a highly modulated field responsive to object manipulations (Figures 5 and S4). In addition, different types of object responses, including LV responses, could often be observed in the same cell across sessions (Figures 5A and S4). The presence of multiple object-related activity changes within the same cell indicates that object response types are not fixed; rather, DG cells have the capacity to exhibit dynamic and flexible responses to object manipulations.

Identification and characterization of putative object-responsive DG cells

To quantify putative object-related changes in individual fields, we identified sessions in which the location of place fields was significantly altered in the MAN sessions. We first identified MAN sessions in which the distance between the location of the manipulated object (either moved or added) and the nearest field was significantly reduced from the STD session (Figures 6A and 6B; STAR Methods). The distance from the manipulated object to the nearest place field decreased more than expected by chance (STAR Methods; Figure 6A) for a significant number of mossy cell session pairs (17 of 157 pairs, 11%; test for proportions $z = 3.35$, $p = 4.03 \times 10^{-4}$), but not for granule cell session pairs (4 out of 54 pairs, 7%; test for proportions $z = 0.81$, $p = 0.21$) (Figure 6A). However, there was no significant difference in the proportion of detected session pairs between cell types ($\chi_{(1)}^2 = 0.52$, $p = 0.47$). Most detected session pairs came from unique cells (15 mossy cells and 4 granule cells). These results indicate that manipulating objects causes a change in the location of firing fields within a subpopulation of DG cells.

Although the preceding analysis can detect multiple types of responses to object manipulation, it is not sensitive to responses without proximal firing to objects (i.e., disappear, trace). Therefore, we compared the spatial correlation values between two

Please cite this article in press as: GoodSmith et al., Flexible encoding of objects and space in single cells of the dentate gyrus, Current Biology (2022), https://doi.org/10.1016/j.cub.2022.01.023

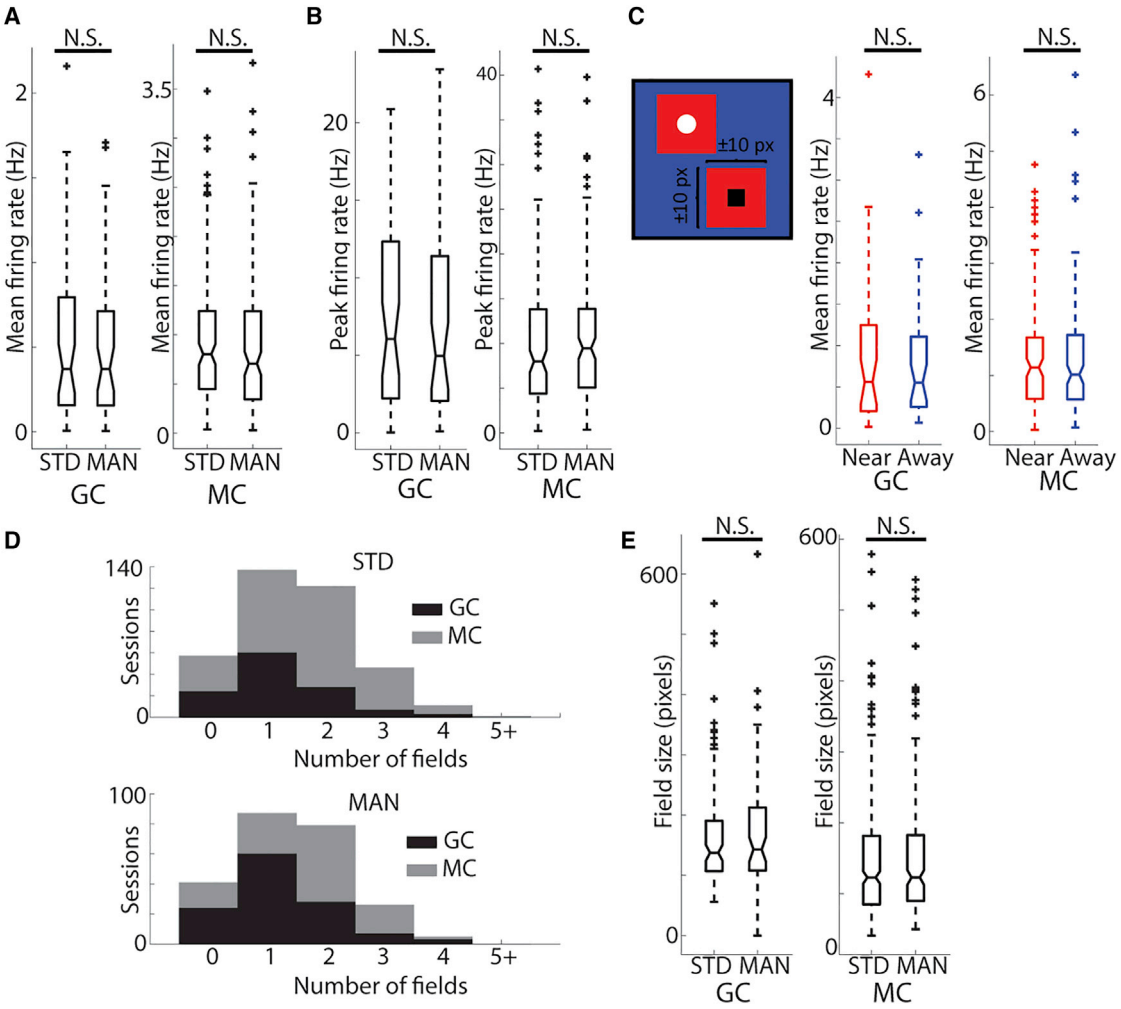

Figure 3. DG population firing rate and place field properties in STD and MAN sessions

(A) Median value of mean firing rates in STD versus MAN sessions for granule cells (left, GC) and mossy cells (right, MC). Results of signed-rank tests are marked above; N.S., not significant; $p > 0.05$.

(B) Same as in (A) but for peak firing rate.

(C) Left: mean firing rate near (red area, $\leq$10 pixels from an object location) or away from (blue area, >10 pixels from all objects) objects. Right: same as in (A) for mean firing rate near versus away from objects for all sessions.

(D) Number of place fields for spatially modulated cells (place field in at least one session). There was no significant difference in the number of fields in STD (top) versus MAN (bottom) sessions for either granule cells (black) or mossy cells (gray). Granule cell histograms are plotted to overlay mossy cell histograms.

(E) Same as in (A) but for place field size (in pixels).

See also Tables S1 and S2.

STD sessions (R_{STD}) with the correlation between STD and MAN sessions (R_{MAN}). There was a significant difference between R_{STD} and R_{MAN} across mossy cells (signed-rank test $z = 2.33$, $p = 0.02$), but not granule cells (signed-rank test $z = 0.40$, $p = 0.69$). There was a subset of individual DG cells, including both granule cells and mossy cells, with a much higher R_{STD} than R_{MAN} (Figures 6C and 6D), which could indicate cells in which object manipulation affected spatial firing. The difference between R_{STD} and R_{MAN} exceeded the 95th percentile of a shuffled distribution (STAR Methods; Figure 6C) for a significant number of mossy cell sessions (23 of 190 session groups, 12%, test for proportions $z = 4.49$, $p = 3.50 \times 10^{-6}$), but not granule cell sessions (4 of 63 session groups, 6%, test for proportions $z = 0.49$, $p = 0.31$; Figure 6C). There was, however, no significant difference in the proportion of mossy cell and granule cell session groups that exceeded the 95th percentile of their respective shuffled distributions ($\chi_{(1)}^2 = 1.64$, $p = 0.20$). Together, these results demonstrate object-related activity in significantly more mossy cells, but not granule cells, than expected by chance; however, there was no significant difference between cell types in the proportion of sessions with significant object-related activity.

In cells with multiple fields, some fields appeared to respond to object manipulations, whereas others appeared unaffected. These stable place fields could produce high rate-map correlation values that would obscure local object-related activity. To address this, we next focused our analysis on the local area

Please cite this article in press as: GoodSmith et al., Flexible encoding of objects and space in single cells of the dentate gyrus, Current Biology (2022), https://doi.org/10.1016/j.cub.2022.01.023

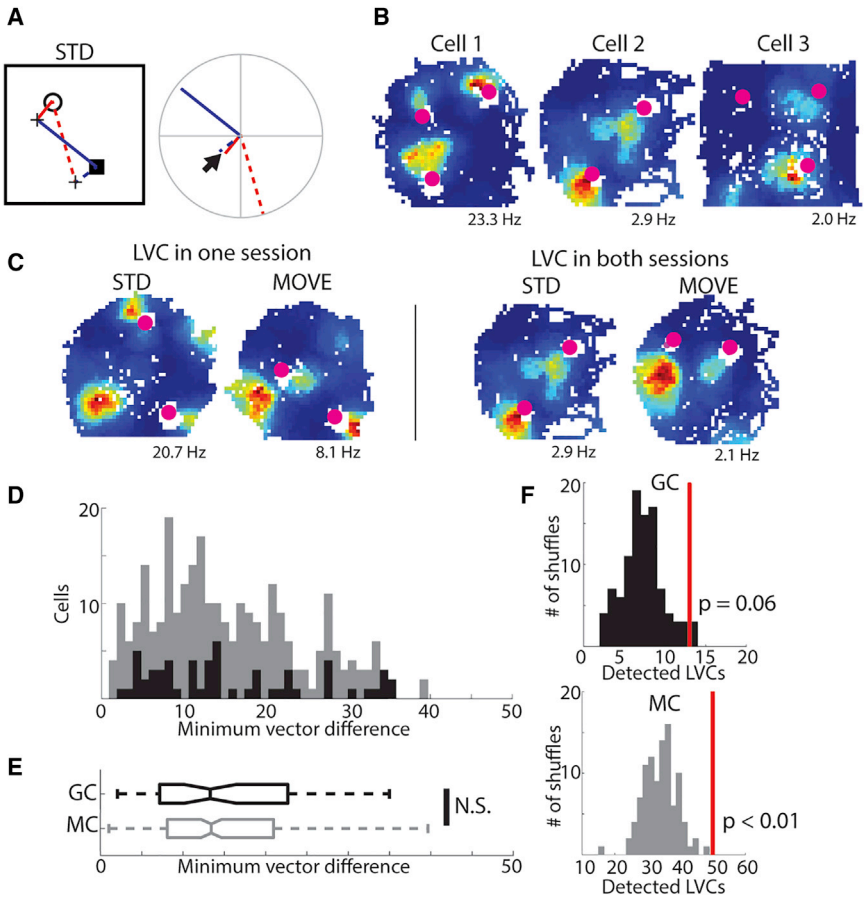

Figure 4. Landmark vector responses

(A) Schematic of the procedure for identifying putative LV responses in a single session. On the left, the vectors between each object (circle and square) and each place field centroid (black "+") are determined (red/blue solid/dashed lines). On the right, the distance and direction from the object are plotted for all vectors (center is object location). The difference is calculated between all pairs of vectors that do not share the same object (same line color) or same place field centroid (same line style). The pair of vectors (that do not share an object or place field) with the smallest difference between them is determined (black arrow). If this minimum vector difference is <7 pixels, the response is considered a LV response.

(B) Example sessions in which the minimum vector difference was <7 pixels (putative LV responses).

(C) Example session pairs (STD and MOVE) detected as LV responses in only the MOVE (left) or both (right) sessions.

(D) Distribution of observed minimum vector difference values for granule cells (black) overlaid over values for mossy cells (gray) (granule cells median 13.49, IQR 7.28–23.01; mossy cells median 13.43, IQR 8.11–20.97; rank-sum test $z = 0.21$, $p = 0.83$).

(E) Boxplot of data from (D).

(F) Random distributions of minimum vector difference values were generated 100 times by randomly assigning place field centers to each session; the number of detected LV responses in each of these 100 random distributions is plotted for granule cells (top, black) and mossy cells (bottom, gray). The red line indicates the number of LV responses observed in our data.

See also Figure S3.

around each object (Figures 6E and 6F). By comparing 21 × 21-pixel segments of firing rate maps based on a fixed spatial area or centered around a manipulated object, we calculated "spatial" and "object-related" correlation values, respectively (STAR Methods). There was a much higher "spatial" than "object-related" correlation value for most cells, indicating the presence of stable place fields. A subset of session pairs, however, had higher "object-related" than "spatial" correlation values (24/124 session pairs; Figure 6E, middle), suggesting that spatial activity was altered by object manipulation. Most session pairs with a higher "object-related" than "spatial" correlation value belonged to mossy cells (21/24, Figure 6E, middle). However, the difference between "object-related" and "spatial" correlation values was not significantly higher for mossy cells than granule cells (granule cell median −0.63, IQR −0.93 to −0.40; mossy cell median −0.53, IQR −0.94 to −0.08; rank-sum test $z = 1.40$, $p = 0.16$; Figure 6E, right). Compared with correlations calculated based on the location of the "unmoved" object (Figure 6E; STAR Methods), the correlation difference values were significantly higher (more "object-related") for the "moved" object than the "unmoved" object for mossy cells (moved median −0.53, IQR −0.94 to −0.08; unmoved median −0.66, IQR −1.0 to −0.27; rank-sum test $z = 2.57$, $p = 0.01$), but not for granule cells (moved median −0.63, IQR −0.93 to −0.40; unmoved median −0.67, IQR −1.05 to −0.19; rank-sum test $z = 0.23$, $p = 0.82$). This result suggests that the population activity of mossy cells, but not granule cells, was significantly altered by object manipulations. A significant proportion of mossy cells (19/94 session pairs; test for proportions $z = 6.77$, $p = 6.55 \times 10^{-12}$), but not granule cells (1/30 session pairs; test for proportions $z = -0.42$, $p = 0.66$), had a correlation difference value that exceeded the 95th percentile of the "unmoved" object distribution (Figure 6E, right). The proportion of cells significantly affected by object manipulation in this analysis was significantly higher for mossy cells than granule cells ($\chi_{(1)}^2 = 4.79$, $p = 0.03$), demonstrating that object-related changes in the local rate map were significantly more common in mossy cells than in granule cells.

Overall, we utilized multiple methods to identify object-related activity in DG cells. Object-related activity was detected more frequently than expected by chance in mossy cells, but not in granule cells. However, in most analyses, there were no significant differences between granule cells and mossy cells in the proportion of sessions with detected object responses. Object-related activity was detected in most animals and at a similar frequency in both male and female mice (Table S1).

DG object responses in distinct environments

We next asked how exposure to distinct environments would affect the object-related activity of DG cells. To determine whether cells displayed consistent object-related activity across environments, we recorded from 3 additional mice as they foraged for food in two environments containing the same

Please cite this article in press as: GoodSmith et al., Flexible encoding of objects and space in single cells of the dentate gyrus, Current Biology (2022), https://doi.org/10.1016/j.cub.2022.01.023

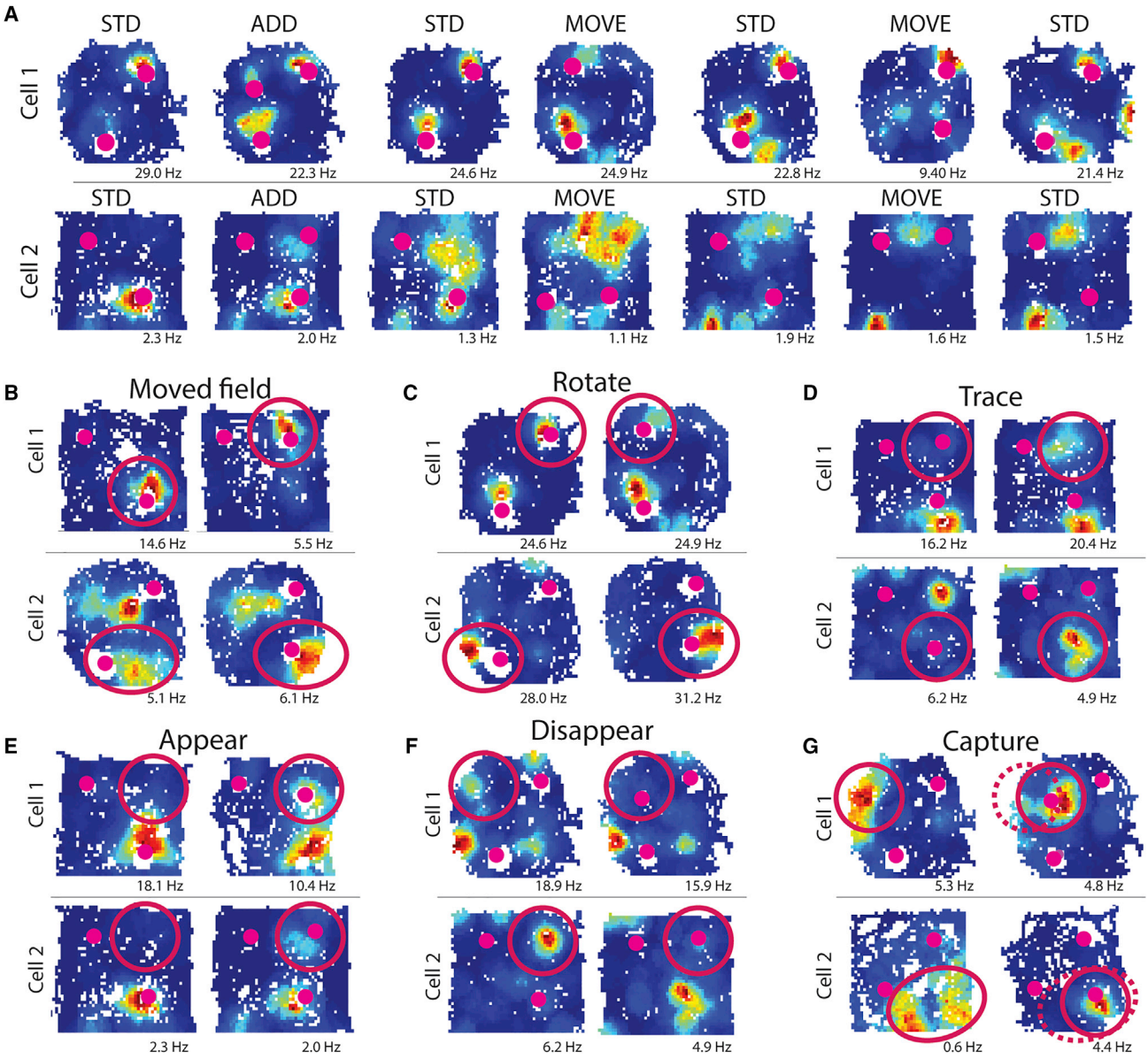

Figure 5. Example object-related DG activity changes

(A) Two example cells with seven recording sessions. Each row is one cell, and the rate map for seven consecutive sessions is shown. Object locations are represented by magenta dots. Diverse object-related changes in activity can be identified in these cells. Cell 1 had multiple fields with the same vector relationship to objects in the first three sessions (putative LV responses). In the next session, a field moved with the moved object but rotated to fire at a new angle relative to the object. In the same session, a new field formed near the unmoved object. When the second object was moved, there were weak fields at both the current and previous locations of that object. In cell 2, a new field formed at the location of an added object and firing persisted at that location throughout the remaining sessions. The stable firing field near the bottom object disappeared when that object was moved.

(B–G) Observed types of object-related activity changes. Two example cells are shown for each type of response, and two consecutive sessions are shown for each cell. Red circles indicate the field with an object-related response. Shown are examples of moved field response (B), rotate response (C), trace response (D), field appears (E), field disappears (F), and capture (G). The dashed red line indicates the prior location of the field.

See also Figure S4.

objects at the same locations (ENV_A and ENV_B; STAR Methods; Figures 7 and S5B).

We recorded from 57 DG cells that had place fields in at least one session through the day (12 granule cells and 45 mossy cells). There were 95 pairs of STD and MOVE sessions (13 granule cell session pairs and 82 mossy cell session pairs) in which at least one field was detected. Most granule cells (11/12) had a place field in only one of the two environments. By contrast, most mossy cells (37/45) had place fields in both environments. For both cell types, the correlation between STD sessions across the two environments was significantly lower than the correlation between repeated STD sessions in the same environment (cells

Please cite this article in press as: GoodSmith et al., Flexible encoding of objects and space in single cells of the dentate gyrus, Current Biology (2022), https://doi.org/10.1016/j.cub.2022.01.023

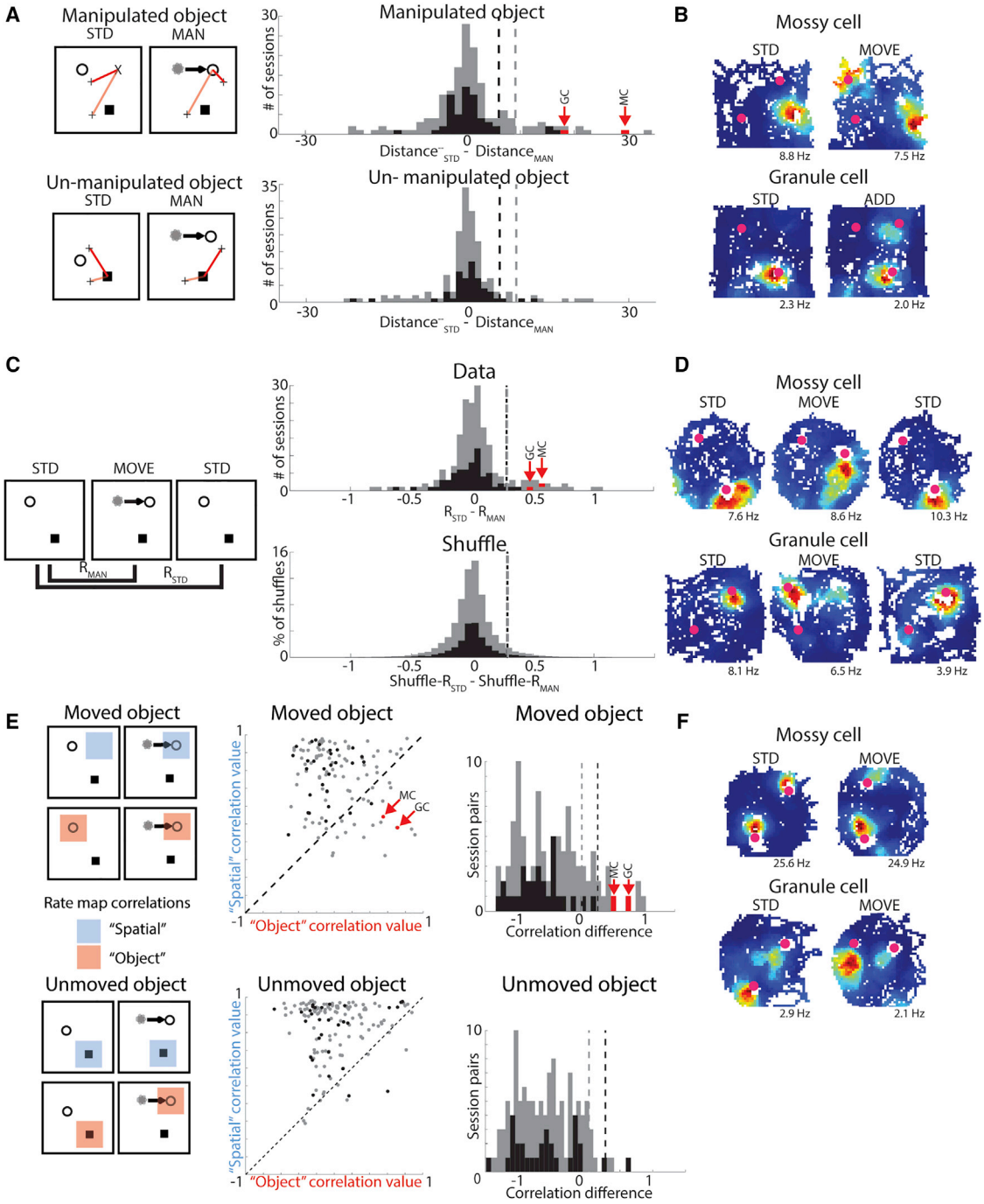

Figure 6. Detection of cells with responses to object manipulation

(A) Distance to nearest place field centroid. Left: schematic of distance calculation in a pair of STD and MAN sessions. The distance (length of the red line) from the location of the moved object ("X" in STD, black circle in MAN) to each place field centroid (black "+") was determined. The shortest distance in each session was determined (dark red line), and the difference between these distances was calculated. Right: distribution of distances between place fields and manipulated object location (top) and unmanipulated object location (bottom).

(B) Spatial firing of example session pairs with a significant reduction in the distance between object location and place field centroid, marked in red in (A).

(C) Rate map correlation difference. Left: schematic of three sequential sessions (STD, MAN, and STD). The correlations between STD sessions (R_{STD}) and between the first STD and MAN session (R_{MAN}) were calculated (granule cells: R_{STD} median 0.77, IQR 0.58–0.86; R_{MAN} median 0.79, IQR 0.57–0.88; signed-rank test $z = 0.40$, $p = 0.69$; mossy cells: R_{STD} median 0.76, IQR 0.57–0.88; and R_{MAN} median 0.73, IQR 0.49–0.85; signed-rank test $z = 2.33$, $p = 0.02$). Right: distribution of correlation difference values between R_{STD} and R_{MAN} for data (top) and shuffled distributions (bottom).

(D) Spatial firing of an example granule cell and mossy cell with significant correlation difference values, marked in red in (C).

(legend continued on next page)

Please cite this article in press as: GoodSmith et al., Flexible encoding of objects and space in single cells of the dentate gyrus, Current Biology (2022), https://doi.org/10.1016/j.cub.2022.01.023

with fields in any STD session; granule cells: rank-sum test $z = 3.83$, $p = 6.28 \times 10^{-5}$; mossy cells: rank-sum test $z = 6.36$, $p = 2.08 \times 10^{-10}$; Figure 7E), even after rotating one rate map in 90° increments (to check for rate map rotations between environments; Figure S5A). These results indicate robust global remapping of DG cells' spatial firing between these contexts. Although individual DG place fields were affected by object manipulations (Figures 7C and 7D), global remapping was only observed in response to changes in the overall environment. This result suggests that although object-related information can be reflected in the activity of individual cells, a stable spatial map of each environment is maintained at the population level.

We next asked whether object responses (i.e., appear, moved field, etc.) were repeated within the same cells across environments to determine whether there was a fixed population of cells with the capacity to respond to objects and/or a fixed response type for individual cells. To evaluate object-related activity changes within each environment, three observers made a subjective assessment of the response to object manipulation (STAR Methods). At least two observers identified the same object-related response type in 92% of the 95 sessions (all three selected the same response for 53% of sessions), indicating reliable identification of object responses. Of all 87 unambiguous (at least two observers identified the same response) sessions with place fields, 43% had spatial firing but no clear object response, and the remaining 57% of sessions were split relatively evenly among other response types (7% move/rotate, 16% appear, 16% disappear, 8% trace, and 10% capture). Of 32 cells with place fields in both environments (31 mossy cells and 1 granule cell), object-related activity changes were observed in only one of the two environments (Figure 7B) for 18 cells (56%, including the single granule cell). In 10 cells (31%), object-related activity changes occurred in both environments. Among the latter group, either a different (6 cells; Figure 7C) or the same (4 cells; Figures 7D and S5C) type of object response was observed in the two environments. An additional 4 cells (12%) had place fields in both environments but had no object-related activity change in either environment (Figure 7F). The proportion of cells with an object response in both environments did not significantly differ from the proportion expected by chance nor did the proportion of cells with the same type of object response in both environments (Table S3). Together, these results indicate that the likelihood of an individual DG cell showing object-related activity following object manipulation is independent in distinct environments and that dedicated DG populations of "object cells" and "spatial cells" are not necessary to convey information about nonspatial cues within a spatial context. Instead, these results suggest that object-related DG activity is context dependent and that different subsets of cells can be object responsive in any given environment.

DISCUSSION

We recorded from DG granule cells and mossy cells as mice freely explored environments to determine whether and how spatial firing properties could be altered by the presence and manipulation of objects. Although most cells maintained a stable, spatial map of the environment, the activity of many DG place cells was affected by the addition or displacement of objects within the environment. Many cells resembled LV cells previously reported in the hippocampus[4,32] (and similar cells in the entorhinal cortex[17]), with multiple firing fields that shared the same vector relationship to multiple objects. Other cells had place fields that moved when a nearby object was moved, fields that appeared, disappeared, rotated, or moved closer to an object, as well as trace firing at previous object locations. These object-related activity changes could be identified in both granule cells and mossy cells, suggesting a similar capacity for object-related activity in both cell types, although it occurred more frequently in the highly active mossy cells. Exposure to a second environment induced global spatial remapping, and cells that responded to object manipulations in one environment were often unaffected by the same manipulations in the other environment, suggesting that DG cells harbor the capacity to flexibly respond to manipulation of objects while maintaining stable spatial representations of distinct environments.

Population-specific properties in the DG

The primary inputs to mossy cells are local cells within the DG.[46] However, mossy cells also receive direct projections from LEC.[47,48] The source of object-related activity in mossy cells is unclear but may reflect a combination of inputs from LEC, granule cells, and CA3 backprojections.[49] Consistent with previous studies,[23,40] most cells that we recorded in the DG (75%) were classified as mossy cells, which often had multiple place fields. Most object-related responses in the present study were identified in mossy cells; furthermore, mossy cells had significantly more object responses than expected by chance in most analyses, which was not the case for granule cells. It is possible that these results reflect a difference in the activation threshold for object-related activity in the two populations. In support of this idea, an object learning task caused mossy cells, but not granule cells, to increase their phase coupling to gamma oscillations associated with LEC inputs,[50] and manipulation of mossy cell activity can impair novel object recognition.[28] Mossy cells, but not granule cells, also showed increased c-Fos expression levels following novel object exposure,[51] and thus, they may be more likely to respond to object manipulations, even with familiar objects.

The prevalence of detected object responses in mossy cells may also reflect differences in intrinsic firing properties between granule cells and mossy cells. Mossy cells are the most active

(E) Local rate map correlation difference. Top: moved object. Bottom: un-moved object. Left: schematics of the location of "object" and "spatial" rate map correlations. Middle: scatterplot of "object" versus "spatial" correlation values (dashed line represents equal "object" and "spatial" correlation). Right: distribution of the difference between "object" and "spatial" correlation values.

(F) Example of session pairs with detected object response, marked in red in (E).

For all plots, mossy cell data are presented in gray, and granule cell data are presented in black, dashed lines reflect the 95th percentile of shuffled or unmanipulated object distributions.

See also Table S1.

Please cite this article in press as: GoodSmith et al., Flexible encoding of objects and space in single cells of the dentate gyrus, Current Biology (2022), https://doi.org/10.1016/j.cub.2022.01.023

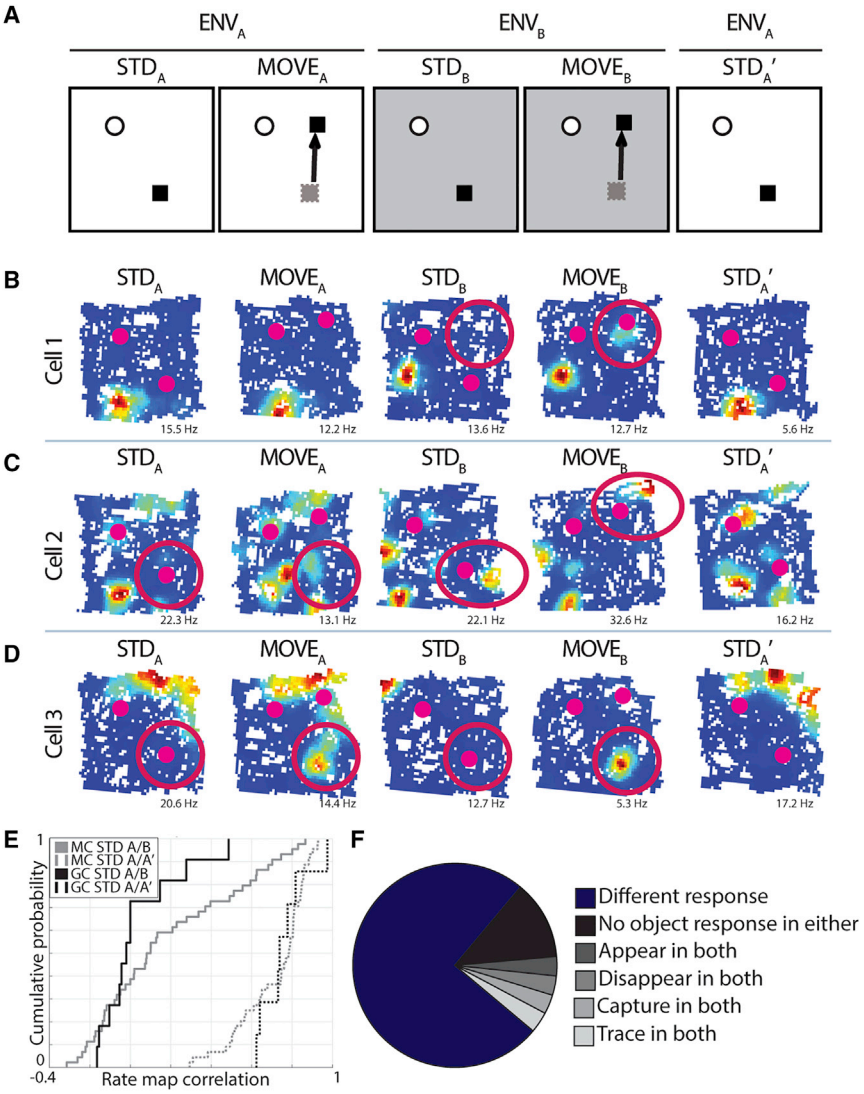

Figure 7. Recordings from two distinct environments

(A) Schematic of recording day. A STD and MOVE session in one environment (ENV_A) were followed by a STD and MOVE session in a second environment (ENV_B). The objects, their locations within the environment, and the manipulation were the same in both environments. The day ended with a final STD session in ENV_A.

(B) Example cell (granule cell) that had no object response in ENV_A but had a field appear in the MOVE session of ENV_B.

(C) Example of a cell (mossy cell) with different object responses in both environments. This cell had a trace field in ENV_A, and a moved field in ENV_B.

(D) Example of a cell (mossy cell) with the same object-related activity in both environments. This cell had a trace response in both ENV_A and ENV_B.

(E) Correlations between STD sessions in the same environment (STD_A versus STD_A') were significantly higher than correlations between different environments (STD_A versus STD_B) (granule cells: STD_A versus STD_B median −0.02, IQR −0.09 to 0.11; STD_A versus STD_A' median 0.74, IQR 0.66–0.81; rank-sum test $z = 3.83$, $p = 6.28 \times 10^{-5}$; mossy cells: STD_A versus STD_B median 0.09, IQR −0.12 to 0.50; STD_A versus STD_A' median 0.78, IQR 0.59–0.84; rank-sum test $z = 6.36$, $p = 2.08 \times 10^{-10}$).

(F) Proportion of all 32 cells that had place fields and had unambiguous activity in both environments. The assigned response to object manipulation was the same in both environments for 8 cells. However, 4 cells did not change their activity following object manipulation in either environment (spatial firing appeared stable) and four had the same object-related change in activity detected in both environments (Figure S5C). The remaining cells had different responses to object manipulation in the two environments.

See also Figure S5 and Table S3.

excitatory cells in the hippocampus, whereas granule cells are the least active. Since we typically observed object-related responses in individual fields, the multiple and frequent place fields of mossy cells increase the odds of detecting an object-related response in this population, even if each granule cell and mossy cell firing field has the same likelihood of responding to a specific object manipulation. Granule cells may form a sparse representation of nonspatial information, similar to their sparse code for space.[37,52,53] Importantly, granule cells could form a robust object/place representation at the population level, even with this very sparse activity. Because mossy cells receive inputs from >100 granule cells,[39] mossy cells could provide a convergent readout for the sparse object-related activity of many granule cell inputs.

In the present study, subjective assessment of DG rate maps revealed clear, but infrequent, object-related activity in classified granule cells. This is consistent with recent studies in head-fixed mice,[32–34,54] in which cue-associated firing was observed in both cell types,[32,33] and odor information could be decoded from granule cell activity,[54] suggesting that both DG cell types represent nonspatial information. In one of these studies, mossy cells encoded cue locations throughout learning, although cue-associated activity in granule cells was more common early in training.[33] The well-trained task used in the present study may have therefore reduced the prevalence of object-related granule cell activity.

Mature granule cells (mGCs) are the most numerous cell type in the DG and presumably the vast majority of the granule cells analyzed in this study, but immature abGCs are added daily.[20] These abGCs receive preferential input from LEC[55,56] and are more excitable and active than mGCs.[57–59] Excitable abGCs have also been implicated in contextual discrimination and object-place learning,[43,60–62] and they may amplify object-related signals from LEC and relay this information to mossy cells and CA3. Intriguingly, abGCs have also been found to monosynaptically inhibit mGCs in response to stimulation of LEC inputs and to activate these cells following MEC input.[63] Therefore, object-related inputs from LEC to abGCs may have the simultaneous

Please cite this article in press as: GoodSmith et al., Flexible encoding of objects and space in single cells of the dentate gyrus, Current Biology (2022), https://doi.org/10.1016/j.cub.2022.01.023

effects of passing an amplified nonspatial signal to mossy cells while inhibiting competing outputs from mGCs. The effects of abGCs on conjunctive object-spatial representations throughout the DG may be assessed in future studies through ablation/inhibition or direct recording of abGCs during exploratory behavior.

Our results suggest that cells in the DG can encode both object and spatial information, but higher-throughput studies may be needed to record from enough cells to resolve the extent of object-related activity in the granule cell population. These types of studies may also reveal influences of the anatomical and functional gradients along the dorsoventral DG axis that are frequently overlooked in studies of DG spatial activity.[51,64–69] Given that the effects of novel object exploration on mossy cell activity are more pronounced in the ventral than dorsal DG,[51,64] there may be a gradient of conjunctive object/space coding in which object information in dorsal DG is strongly tied to defined spatial firing locations, whereas ventral DG activity is less spatially modulated and more sensitive to object novelty. Furthermore, the DG contains a diverse population of interneurons[70,71] that regulates activity throughout the DG, and their role in shaping object-related DG activity will require further study and analysis. Finally, despite robust object-related activity in the DG, it is important to note that most cells had stable place fields that were unaffected by our object manipulations. It is possible that many of these cells still reflect nonspatial information but were driven by stable cues rather than the manipulated objects.

Beyond the DG, representations of object and space are likely linked throughout the hippocampus and its input streams. Objects and cues are important to defining the spatial layout of the environment, and manipulation of hippocampal activity affects object recognition and object-place learning.[72–74] Some of the same types of object-related activity we report here have been observed in other hippocampal regions, such as the LV responses reported in CA1 and CA3.[2–4,6,75–77] In contrast to activity changes associated with a single object, LV responses could reflect a mechanism to link the overall geometric relationships between multiple objects and environment boundaries.[78] How these types of object-related activity are processed and utilized within each hippocampal subfield is unclear. The DG may produce conjunctive representations, but the extent to which they are preserved in CA1 is also unclear[3,72,75] and may rely on task demands, similar to the recent finding that activity decorrelation in CA1, but not DG, reflects behavioral discrimination.[79] The DG may participate in a functional pattern separation circuit that is closely associated with distal CA1,[80] which receives preferential LEC inputs and displays more object-related activity.[76,81–83] Conjunctive object-place associations in the DG would support the capacity of this circuit to discriminate between similar experiences that occur within the same environment, which is critical for the formation and storage of episodic memories.

Conjunctive encoding of spatial and nonspatial information

The DG is believed to be necessary for the conjunctive encoding of the allocentric context (predominantly from MEC) and egocentric content (predominantly from LEC) of an experience into a cohesive representation.[14–16,30,31,84,85] Behavioral studies have provided support for the role of the DG in forming complex associations between objects, sensory cues, and spatial locations.[22,26,27,84,86] However, it is unclear how the activity of cells in the DG may reflect these conjunctive representations. Conjunctive encoding could be an emergent property of the DG as a whole, arising from distinct populations of dedicated DG "place" cells and "object" cells that process spatial and nonspatial information in parallel[34] for integration downstream of the DG.[4,75] However, there is already considerable cross-talk between spatial and nonspatial inputs to the DG, both within and upstream of the entorhinal cortex.[45,87–89] Although LEC and MEC are often viewed as providing nonspatial and spatial information, respectively, to the hippocampus,[45,90] recent studies have identified object-vector cells in MEC[17] and egocentric[15] and spatial representations in LEC,[44,45] suggesting some overlap of object and spatial information in afferent projections to the DG. It is therefore possible that conjunctive object-spatial representations do not originate in the DG but are inherited from upstream inputs. Selective inhibition of inputs could reveal MEC- or LEC-specific contributions to object-related DG activity.

A strict definition of conjunctive encoding is often used to describe cells that exhibit stereotyped activity when multiple conditions are met, such as grid × head direction cells that fire when the animal is in a specific spatial location and is facing a specific direction.[91] Similarly, a conjunctive object-place cell might be expected to fire only in response to a particular object-place configuration. This level of specificity would suggest that small changes to object location or identity could induce global remapping across a population of cells with strictly conjunctive responses. In this study, we typically did not see this type of conjunctive representation in object-responsive place fields. Although individual fields that appear or disappear could reflect a purely conjunctive representation, most object-related responses that we observed also track with the object location. Together, our results suggest that conjunctive encoding can occur through the aggregated responses of individual fields to object manipulations and multiplexing of object and spatial information within the same cell.

Although individual fields in a subset of DG cells are modulated by object manipulations, we observed global remapping across the population upon exposure to a second environment. Object manipulation affected the activity of different subsets of DG cells in each environment; the same DG cell that had a clear object response in one environment could be unaffected by the same manipulation in another environment. Thus, there appears to be a threshold for DG responses, wherein small local changes can induce field-specific modulation of spatial firing but changes in the spatial context induce global remapping, as well as the recruitment of a new set of object-associated cells. This result suggests that the population of object-responsive cells can be reassigned in a context-dependent manner and that there is not a dedicated population of "object cells." Instead, our data reveal flexibility in the subset of cells that are object responsive in different contexts, the type(s) of object responses in single cells across sessions, and the response of individual fields to object manipulation within single cells. Our results suggest that spatial and nonspatial information can be integrated and dynamically modulated in response to environmental manipulations by the DG.

Place cells have been proposed to provide a spatial framework for an internal cognitive map.[10] Information about events

and experiences can be encoded onto that spatial map to guide spatial navigation and episodic memory.[10] To distinguish among experiences in different places, it is advantageous to encode each distinct environment as a separate spatial map with minimal overlap. However, within the same spatial environment, cues and objects can change over time. Multiple experiences in the same environment will have slightly different cues, and the ability to flexibly represent such changes without a complete reorganization of the spatial representation is essential. We found that the granule cell and mossy cell populations in the DG formed stable spatial representations while flexibly responding to object manipulations, which would support the encoding of unique experiences within the same environment.

STAR★METHODS

Detailed methods are provided in the online version of this paper and include the following:

- KEY RESOURCES TABLE
- RESOURCE AVAILABILITY
  - Lead contact
  - Materials availability
  - Data and code availability
- EXPERIMENTAL MODEL AND SUBJECT DETAILS
- METHOD DETAILS
  - Surgical procedures
  - Training and Behavior
  - Electrophysiological recordings
  - Histological procedures
  - Unit isolation
  - Rate maps and place fields
- QUANTIFICATION AND STATISTICAL ANALYSIS
  - Cell type classification
  - Landmark vector analysis
  - Distance to nearest place field
  - Rate map correlation analysis
  - Subjective response type evaluation
  - Statistical tests

SUPPLEMENTAL INFORMATION

Supplemental information can be found online at https://doi.org/10.1016/j.cub.2022.01.023.

ACKNOWLEDGMENTS

We thank B. Temsamrit, E. LaNoce, A. Garcia, and A. Angelucci for technical support and lab coordination, and Francesco Savelli for feedback on the manuscript. This work was supported by grants from the National Institutes of Health (R01NS039456 to J.J.K., R35NS116843 to H.S., and R35NS097370 to G.-l.M.).

AUTHOR CONTRIBUTIONS

D.G., J.J.K., and K.M.C. designed the experiments; D.G. and S.H.K. collected the data; D.G., K.M.C., S.H.K., and V.P. analyzed the data; H.S., G.-l.M., J.J.K., and K.M.C. provided supervision and funding; D.G. and K.M.C. wrote the initial draft of the manuscript; and all authors provided comments and feedback on the manuscript.

DECLARATION OF INTERESTS

The authors declare no competing financial interests.

Received: June 25, 2021
Revised: November 12, 2021
Accepted: January 10, 2022
Published: February 1, 2022

REFERENCES

1. Moita, M.A.P., Rosis, S., Zhou, Y., LeDoux, J.E., and Blair, H.T. (2003). Hippocampal place cells acquire location-specific responses to the conditioned stimulus during auditory fear conditioning. Neuron *37*, 485–497.
2. Komorowski, R.W., Manns, J.R., and Eichenbaum, H. (2009). Robust conjunctive item-place coding by hippocampal neurons parallels learning what happens where. J. Neurosci. *29*, 9918–9929.
3. Manns, J.R., and Eichenbaum, H. (2009). A cognitive map for object memory in the hippocampus. Learn. Mem. *16*, 616–624.
4. Deshmukh, S.S., and Knierim, J.J. (2013). Influence of local objects on hippocampal representations: landmark vectors and memory. Hippocampus *23*, 253–267.
5. Geiller, T., Fattahi, M., Choi, J.S., and Royer, S. (2017). Place cells are more strongly tied to landmarks in deep than in superficial CA1. Nat. Commun. *8*, 14531.
6. Burke, S.N., Maurer, A.P., Nematollahi, S., Uprety, A.R., Wallace, J.L., and Barnes, C.A. (2011). The influence of objects on place field expression and size in distal hippocampal CA1. Hippocampus *21*, 783–801.
7. Rivard, B., Li, Y., Lenck-Santini, P.-P., Poucet, B., and Muller, R.U. (2004). Representation of objects in space by two classes of hippocampal pyramidal cells. J. Gen. Physiol. *124*, 9–25.
8. Lenck-Santini, P.-P., Rivard, B., Muller, R.U., and Poucet, B. (2005). Study of CA1 place cell activity and exploratory behavior following spatial and nonspatial changes in the environment. Hippocampus *15*, 356–369.
9. O'Keefe, J. (1976). Place units in the hippocampus of the freely moving rat. Exp. Neurol. *51*, 78–109.
10. O'Keefe, J., and Nadel, L. (1978). The Hippocampus as a Cognitive Map (Clarendon Press).
11. Gaffan, D. (1998). Idiothetic input into object-place configuration as the contribution to memory of the monkey and human hippocampus: a review. Exp. Brain Res. *123*, 201–209.
12. Suzuki, W.A., Miller, E.K., and Desimone, R. (1997). Object and place memory in the macaque entorhinal cortex. J. Neurophysiol. *78*, 1062–1081.
13. Rolls, E.T., Xiang, J., and Franco, L. (2005). Object, space, and object-space representations in the primate hippocampus. J. Neurophysiol. *94*, 833–844.
14. Lisman, J.E. (2007). Role of the dual entorhinal inputs to hippocampus: a hypothesis based on cue/action (non-self/self) couplets. Prog. Brain Res. *163*, 615–625.
15. Wang, C., Chen, X., Lee, H., Deshmukh, S.S., Yoganarasimha, D., Savelli, F., and Knierim, J.J. (2018). Egocentric coding of external items in the lateral entorhinal cortex. Science *362*, 945–949.
16. Wang, C., Chen, X., and Knierim, J.J. (2020). Egocentric and allocentric representations of space in the rodent brain. Curr. Opin. Neurobiol. *60*, 12–20.
17. Høydal, Ø.A., Skytøen, E.R., Andersson, S.O., Moser, M.-B., and Moser, E.I. (2019). Object-vector coding in the medial entorhinal cortex. Nature *568*, 400–404.
18. Amaral, D.G., Scharfman, H.E., and Lavenex, P. (2007). The dentate gyrus: fundamental neuroanatomical organization (dentate gyrus for dummies). Prog. Brain Res. *163*, 3–22.
19. Scharfman, H.E. (2016). The enigmatic mossy cell of the dentate gyrus. Nat. Rev. Neurosci. *17*, 562–575.

20. Ming, G.L., and Song, H. (2011). Adult neurogenesis in the mammalian brain: significant answers and significant questions. Neuron *70*, 687–702.
21. Jinde, S., Zsiros, V., Jiang, Z., Nakao, K., Pickel, J., Kohno, K., Belforte, J.E., and Nakazawa, K. (2012). Hilar mossy cell degeneration causes transient dentate granule cell hyperexcitability and impaired pattern separation. Neuron *76*, 1189–1200.
22. Bui, A.D., Nguyen, T.M., Limouse, C., Kim, H.K., Szabo, G.G., Felong, S., Maroso, M., and Soltesz, I. (2018). Dentate gyrus mossy cells control spontaneous convulsive seizures and spatial memory. Science *359*, 787–790.
23. GoodSmith, D., Lee, H., Neunuebel, J.P., Song, H., and Knierim, J.J. (2019). Dentate gyrus mossy cells share a role in pattern separation with dentate granule cells and proximal CA3 pyramidal cells. J. Neurosci. *39*, 9570–9584.
24. Myers, C.E., and Scharfman, H.E. (2009). A role for hilar cells in pattern separation in the dentate gyrus: a computational approach. Hippocampus *19*, 321–337.
25. Kesner, R.P., Taylor, J.O., Hoge, J., and Andy, F. (2015). Role of the dentate gyrus in mediating object-spatial configuration recognition. Neurobiol. Learn. Mem. *118*, 42–48.
26. Lee, I., and Solivan, F. (2010). Dentate gyrus is necessary for disambiguating similar object-place representations. Learn. Mem. *17*, 252–258.
27. Morris, A.M., Weeden, C.S., Churchwell, J.C., and Kesner, R.P. (2013). The role of the dentate gyrus in the formation of contextual representations. Hippocampus *23*, 162–168.
28. Botterill, J.J., Vinod, K.Y., Gerencer, K.J., Teixeira, C.M., LaFrancois, J.J., and Scharfman, H.E. (2021). Bidirectional regulation of cognitive and anxiety-like behaviors by dentate gyrus mossy cells in male and female mice. J. Neurosci. *41*, 2475–2495.
29. Kesner, R.P. (2007). A behavioral analysis of dentate gyrus function. Prog. Brain Res. *163*, 567–576.
30. Lee, J.W., and Jung, M.W. (2017). Separation or binding? Role of the dentate gyrus in hippocampal mnemonic processing. Neurosci. Biobehav. Rev. *75*, 183–194.
31. Knierim, J.J., Lee, I., and Hargreaves, E.L. (2006). Hippocampal place cells: parallel input streams, subregional processing, and implications for episodic memory. Hippocampus *16*, 755–764.
32. Kim, S., Jung, D., and Royer, S. (2020). Place cell maps slowly develop via competitive learning and conjunctive coding in the dentate gyrus. Nat. Commun. *11*, 4550.
33. Jung, D., Kim, S., Sariev, A., Sharif, F., Kim, D., and Royer, S. (2019). Dentate granule and mossy cells exhibit distinct spatiotemporal responses to local change in a one-dimensional landscape of visual-tactile cues. Sci. Rep. *9*, 9545.
34. Tuncdemir, S.N., Grosmark, A.D., Turi, G.F., Shank, A., Bowler, J.C., Ordek, G., et al. (2022). Parallel processing of sensory cue and spatial information in the dentate gyrus. Cell Rep. *38*, 110257.
35. Vogel-Ciernia, A., and Wood, M.A. (2014). Examining object location and object recognition memory in mice. Curr. Protoc. Neurosci. *69*, 8–31, 1–8.31.17.
36. Kesner, R.P. (2018). An analysis of dentate gyrus function (an update). Behav. Brain Res. *354*, 84–91.
37. GoodSmith, D., Chen, X., Wang, C., Kim, S.H., Song, H., Burgalossi, A., et al. (2017). Spatial representations of granule cells and mossy cells of the dentate gyrus. Neuron *93*, 677–690, e5.
38. Senzai, Y., and Buzsáki, G. (2017). Physiological properties and behavioral correlates of hippocampal granule cells and mossy cells. Neuron *93*, 691–704, e5.
39. Henze, D.A., and Buzsáki, G. (2007). Hilar mossy cells: functional identification and activity in vivo. Prog. Brain Res. *163*, 199–216.
40. Neunuebel, J.P., and Knierim, J.J. (2012). Spatial firing correlates of physiologically distinct cell types of the rat dentate gyrus. J. Neurosci. *32*, 3848–3858.
41. Danielson, N.B., Turi, G.F., Ladow, M., Chavlis, S., Petrantonakis, P.C., Poirazi, P., and Losonczy, A. (2017). In vivo imaging of dentate gyrus mossy cells in behaving mice. Neuron *93*, 552–559, e4.
42. Diamantaki, M., Frey, M., Berens, P., Preston-Ferrer, P., and Burgalossi, A. (2016). Sparse activity of identified dentate granule cells during spatial exploration. eLife *5*, 1109–1123.
43. Danielson, N.B., Kaifosh, P., Zaremba, J.D., Lovett-Barron, M., Tsai, J., Denny, C.A., Balough, E.M., Goldberg, A.R., Drew, L.J., Hen, R., et al. (2016). Distinct contribution of adult-born hippocampal granule cells to context encoding. Neuron *90*, 101–112.
44. Tsao, A., Moser, M.-B., and Moser, E.I. (2013). Traces of experience in the lateral entorhinal cortex. Curr. Biol. *23*, 399–405.
45. Deshmukh, S.S., and Knierim, J.J. (2011). Representation of non-spatial and spatial information in the lateral entorhinal cortex. Front. Behav. Neurosci. *5*, 69.
46. Scharfman, H.E., and Myers, C.E. (2013). Hilar mossy cells of the dentate gyrus: a historical perspective. Front. Neural Circuits *6*, 106.
47. Azevedo, E.P., Pomeranz, L., Cheng, J., Schneeberger, M., Vaughan, R., Stern, S.A., Tan, B., Doerig, K., Greengard, P., and Friedman, J.M. (2019). A role of Drd2 hippocampal neurons in context-dependent food intake. Neuron *102*, 873–886, e5.
48. Scharfman, H.E. (1991). Dentate hilar cells with dendrites in the molecular layer have lower thresholds for synaptic activation by perforant path than granule cells. J. Neurosci. *11*, 1660–1673.
49. Scharfman, H.E. (2007). The CA3 "backprojection" to the dentate gyrus. Prog. Brain Res. *163*, 627–637.
50. Fernández-Ruiz, A., Oliva, A., Soula, M., Rocha-Almeida, F., Nagy, G.A., Martin-Vazquez, G., and Buzsáki, G. (2021). Gamma rhythm communication between entorhinal cortex and dentate gyrus neuronal assemblies. Science *372*, eabf3119.
51. Bernstein, H.L., Lu, Y.-L., Botterill, J.J., and Scharfman, H.E. (2019). Novelty and novel objects increase c-Fos immunoreactivity in mossy cells in the mouse dentate gyrus. Neural Plast *2019*, 1815371.
52. Chawla, M.K., Guzowski, J.F., Ramirez-Amaya, V., Lipa, P., Hoffman, K.L., Marriott, L.K., Worley, P.F., McNaughton, B.L., and Barnes, C.A. (2005). Sparse, environmentally selective expression of Arc RNA in the upper blade of the rodent fascia dentata by brief spatial experience. Hippocampus *15*, 579–586.
53. Hainmueller, T., and Bartos, M. (2018). Parallel emergence of stable and dynamic memory engrams in the hippocampus. Nature *558*, 292–296.
54. Woods, N.I., Stefanini, F., Apodaca-Montano, D.L., Tan, I.M.C., Biane, J.S., and Kheirbek, M.A. (2020). The dentate gyrus classifies cortical representations of learned stimuli. Neuron *107*, 173–184, e6.
55. Vivar, C., Potter, M.C., Choi, J., Lee, J.-Y., Stringer, T.P., Callaway, E.M., Gage, F.H., Suh, H., and van Praag, H. (2012). Monosynaptic inputs to new neurons in the dentate gyrus. Nat. Commun. *3*, 1107.
56. Woods, N.I., Vaaga, C.E., Chatzi, C., Adelson, J.D., Collie, M.F., Perederiy, J.V., Tovar, K.R., and Westbrook, G.L. (2018). Preferential targeting of lateral entorhinal inputs onto newly integrated granule cells. J. Neurosci. *38*, 5843–5853.
57. Ge, S., Yang, C.-H., Hsu, K.-S., Ming, G.-L., and Song, H. (2007). A critical period for enhanced synaptic plasticity in newly generated neurons of the adult brain. Neuron *54*, 559–566.
58. Schmidt-Hieber, C., Jonas, P., and Bischofberger, J. (2004). Enhanced synaptic plasticity in newly generated granule cells of the adult hippocampus. Nature *429*, 184–187.
59. Marín-Burgin, A., Mongiat, L.A., Pardi, M.B., and Schinder, A.F. (2012). Unique processing during a period of high excitation/inhibition balance in adult-born neurons. Science *335*, 1238–1242.
60. Tuncdemir, S.N., Lacefield, C.O., and Hen, R. (2019). Contributions of adult neurogenesis to dentate gyrus network activity and computations. Behav. Brain Res. *374*, 112112.
61. Sahay, A., Scobie, K.N., Hill, A.S., O'Carroll, C.M., Kheirbek, M.A., Burghardt, N.S., Fenton, A.A., Dranovsky, A., and Hen, R. (2011).

Increasing adult hippocampal neurogenesis is sufficient to improve pattern separation. Nature *472*, 466–470.

62. Madsen, T.M., Kristjansen, P.E.G., Bolwig, T.G., and Wörtwein, G. (2003). Arrested neuronal proliferation and impaired hippocampal function following fractionated brain irradiation in the adult rat. Neuroscience *119*, 635–642.
63. Luna, V.M., Anacker, C., Burghardt, N.S., Khandaker, H., Andreu, V., Millette, A., Leary, P., Ravenelle, R., Jimenez, J.C., Mastrodonato, A., et al. (2019). Adult-born hippocampal neurons bidirectionally modulate entorhinal inputs into the dentate gyrus. Science *364*, 578–583.
64. Fredes, F., Silva, M.A., Koppensteiner, P., Kobayashi, K., Joesch, M., and Shigemoto, R. (2021). Ventro-dorsal hippocampal pathway gates novelty-induced contextual memory formation. Curr. Biol. *31*, 25–38, e5.
65. Botterill, J.J., Gerencer, K.J., Vinod, K.Y., Alcantara-Gonzalez, D., and Scharfman, H.E. (2021). Dorsal and ventral mossy cells differ in their axonal projections throughout the dentate gyrus of the mouse hippocampus. Hippocampus *31*, 522–539.
66. Duffy, A.M., Schaner, M.J., Chin, J., and Scharfman, H.E. (2013). Expression of c-fos in hilar mossy cells of the dentate gyrus in vivo. Hippocampus *23*, 649–655.
67. Houser, C.R., Peng, Z., Wei, X., Huang, C.S., and Mody, I. (2021). Mossy cells in the dorsal and ventral dentate gyrus differ in their patterns of axonal projections. J. Neurosci. *41*, 991–1004.
68. Jinno, S., Ishizuka, S., and Kosaka, T. (2003). Ionic currents underlying rhythmic bursting of ventral mossy cells in the developing mouse dentate gyrus. Eur. J. Neurosci. *17*, 1338–1354.
69. Kheirbek, M.A., Drew, L.J., Burghardt, N.S., Costantini, D.O., Tannenholz, L., Ahmari, S.E., Zeng, H., Fenton, A.A., and Hen, R. (2013). Differential control of learning and anxiety along the dorsoventral axis of the dentate gyrus. Neuron *77*, 955–968.
70. Sik, A., Penttonen, M., and Buzsáki, G. (1997). Interneurons in the hippocampal dentate gyrus: an in vivo intracellular study. Eur. J. Neurosci. *9*, 573–588.
71. Morgan, R.J., Santhakumar, V., and Soltesz, I. (2007). Modeling the dentate gyrus. Prog. Brain Res. *163*, 639–658.
72. Cohen, S.J., Munchow, A.H., Rios, L.M., Zhang, G., Ásgeirsdóttir, H.N., and Stackman, R.W., Jr. (2013). The rodent hippocampus is essential for nonspatial object memory. Curr. Biol. *23*, 1685–1690.
73. Lee, I., and Solivan, F. (2008). The roles of the medial prefrontal cortex and hippocampus in a spatial paired-association task. Learn. Mem. *15*, 357–367.
74. Gilbert, P.E., and Kesner, R.P. (2002). Role of the rodent hippocampus in paired-associate learning involving associations between a stimulus and a spatial location. Behav. Neurosci. *116*, 63–71.
75. Ásgeirsdóttir, H.N., Cohen, S.J., and Stackman, R.W., Jr. (2020). Object and place information processing by CA1 hippocampal neurons of C57BL/6J mice. J. Neurophysiol. *123*, 1247–1264.
76. Vandrey, B., Duncan, S., and Ainge, J.A. (2021). Object and object-memory representations across the proximodistal axis of CA1. Hippocampus *31*, 881–896.
77. Sarel, A., Finkelstein, A., Las, L., and Ulanovsky, N. (2017). Vectorial representation of spatial goals in the hippocampus of bats. Science *355*, 176–180.
78. Bicanski, A., and Burgess, N. (2019). A computational model of visual recognition memory via grid cells. Curr. Biol. *29*, 979–990, e4.
79. Allegra, M., Posani, L., Gómez-Ocádiz, R., and Schmidt-Hieber, C. (2020). Differential relation between neuronal and behavioral discrimination during hippocampal memory encoding. Neuron *108*, 1103–1112, e6.
80. Lee, H., GoodSmith, D., and Knierim, J.J. (2020). Parallel processing streams in the hippocampus. Curr. Opin. Neurobiol. *64*, 127–134.
81. Naber, P.A., Lopes da Silva, F.H., and Witter, M.P. (2001). Reciprocal connections between the entorhinal cortex and hippocampal fields CA1 and the subiculum are in register with the projections from CA1 to the subiculum. Hippocampus *11*, 99–104.
82. Nakazawa, Y., Pevzner, A., Tanaka, K.Z., and Wiltgen, B.J. (2016). Memory retrieval along the proximodistal axis of CA1. Hippocampus *26*, 1140–1148.
83. Ito, H.T., and Schuman, E.M. (2012). Functional division of hippocampal area CA1 via modulatory gating of entorhinal cortical inputs. Hippocampus *22*, 372–387.
84. Hunsaker, M.R., Mooy, G.G., Swift, J.S., and Kesner, R.P. (2007). Dissociations of the medial and lateral perforant path projections into dorsal DG, CA3, and CA1 for spatial and nonspatial (visual object) information processing. Behav. Neurosci. *121*, 742–750.
85. Kesner, R.P. (2013). An analysis of the dentate gyrus function. Behav. Brain Res. *254*, 1–7.
86. Lee, J.W., Kim, W.R., Sun, W., and Jung, M.W. (2012). Disruption of dentate gyrus blocks effect of visual input on spatial firing of CA1 neurons. J. Neurosci. *32*, 12999–13003.
87. Furtak, S.C., Ahmed, O.J., and Burwell, R.D. (2012). Single neuron activity and theta modulation in postrhinal cortex during visual object discrimination. Neuron *76*, 976–988.
88. Burwell, R.D. (2000). The parahippocampal region: corticocortical connectivity. Ann. NY Acad. Sci. *911*, 25–42.
89. Miranda, M., Kent, B.A., Morici, J.F., Gallo, F., Saksida, L.M., Bussey, T.J., Weisstaub, N., and Bekinschtein, P. (2018). NMDA receptors and BDNF are necessary for discrimination of overlapping spatial and non-spatial memories in perirhinal cortex and hippocampus. Neurobiol. Learn. Mem. *155*, 337–343.
90. Hargreaves, E.L., Rao, G., Lee, I., and Knierim, J.J. (2005). Major dissociation between medial and lateral entorhinal input to dorsal hippocampus. Science *308*, 1792–1794.
91. Sargolini, F., Fyhn, M., Hafting, T., McNaughton, B.L., Witter, M.P., Moser, M.B., and Moser, E.I. (2006). Conjunctive representation of position, direction, and velocity in entorhinal cortex. Science *312*, 758–762.
92. Breiman, L. (2001). Random forests. Mach. Learn. *45*, 5–32.
93. Liaw, A., and Wiener, M. (2002). Classification and regression by randomForest. R News *2*, 18–22.
94. Berg, D.A., Yoon, K.-J., Will, B., Xiao, A.Y., Kim, N.-S., Christian, K.M., Song, H., and Ming, G.L. (2015). Tbr2-expressing intermediate progenitor cells in the adult mouse hippocampus are unipotent neuronal precursors with limited amplification capacity under homeostasis. Front. Biol. *10*, 262–271.
95. Kloosterman, F., Davidson, T.J., Gomperts, S.N., Layton, S.P., Hale, G., Nguyen, D.P., and Wilson, M.A. (2009). Micro-drive array for chronic in vivo recording: drive fabrication. J. Vis. Exp. (26)e1094
96. Skaggs, W.E., McNaughton, B.L., Wilson, M.A., and Barnes, C.A. (1996). Theta phase precession in hippocampal neuronal populations and the compression of temporal sequences. Hippocampus *6*, 149–172.
97. Houser, C.R. (2007). Interneurons of the dentate gyrus: an overview of cell types, terminal fields and neurochemical identity. Prog. Brain Res. *163*, 217–232.
98. Kentros, C.G., Agnihotri, N.T., Streater, S., Hawkins, R.D., and Kandel, E.R. (2004). Increased attention to spatial context increases both place field stability and spatial memory. Neuron *42*, 283–295.

Please cite this article in press as: GoodSmith et al., Flexible encoding of objects and space in single cells of the dentate gyrus, Current Biology (2022), https://doi.org/10.1016/j.cub.2022.01.023

STAR★METHODS

KEY RESOURCES TABLE

REAGENT or RESOURCE	SOURCE	IDENTIFIER
Dataset used in the current study	N/A	GitHub: https://github.com/dgoodsmith/GoodSmithKim_DGobject2022
Matlab	Mathworks	https://www.mathworks.com/products/matlab
Random Forests	Breiman [92] and Liaw and Wiener[93]	https://code.google.com/archive/p/randomforest-matlab/
Cheetah acquisition software	Neuralynx	https://neuralynx.com/
Digital Lynx SX data acquisition system	Neuralynx	https://neuralynx.com/
VECTASHIELD Mounting medium with DAPI	Vector Laboratories	Cat#H-1500; RRID: AB_236788

RESOURCE AVAILABILITY

Lead contact

Requests for further information, data, and other resources can be directed to the lead contact, Kimberly M. Christian (kchristi@pennmedicine.upenn.edu)

Materials availability

This study did not generate new materials

Data and code availability

Raw data collected in this study are extremely large files and not feasible for upload to an online repository but are available upon request to the lead contact. The processed data used in this study are available on GitHub (GitHub: https://github.com/dgoodsmith/GoodSmithKim_DGobject2022).

EXPERIMENTAL MODEL AND SUBJECT DETAILS

We recorded from 21 Tbr2-CreER^{T2}::ChR2$^{f/f}$ mice[94] (13 male, 8 female, 19–29 g, 10–23 weeks old, C57BL/6 background). These mice were used to express Channelrhodopsin (ChR2) in a birth-dated population of adult-born immature granule cells (for a different study). Mice were implanted with a custom-designed recording drive,[95] consisting of seven independently movable tetrodes, one movable reference tetrode, and one fixed 200 μm diameter optic fiber. The optic fiber was used for another experiment and ended well above DG (targeted to end above the CA1 pyramidal cell layer, 1-1.5 mm below the brain surface). Mice were group housed prior to surgery and individually housed after surgery on a 12 hr light/dark cycle with ad libitum access to water. Both male and female mice were used. All surgeries and animal procedures complied with National Institutes of Health guidelines and were approved by the Institutional Animal Care and Use Committees at Johns Hopkins University and the University of Pennsylvania.

METHOD DETAILS

Surgical procedures

During surgery, mice were anesthetized with isoflurane or a mixture of ketamine/xylazine/acepromazine (70-100, 5-12, and 1-3 mg/kg, respectively). A surgical plane was maintained with supplemental ketamine/xylazine/acepromazine or with isoflurane (to effect). The skull was exposed and cleaned, and a craniotomy was drilled. The dura was cut, and the drive was positioned so that the fiber (center of the diamond-shaped bundle) was located 1.3 mm medial and 2.0 mm posterior to bregma. A ground screw was placed above the cerebellum, and 2-3 additional anchor screws were added to the skull (positioned so as to not interfere with drive implantation). The craniotomy was sealed with Kwik-Sil (World Precision Instruments), and the drive was secured to the skull with Metabond (Parkell).

Training and Behavior

After mice had recovered from surgery, they were food restricted to ~80-90% of their free-feeding weight and trained to forage for chocolate sprinkles in a series of distinct environments. Mice were trained in 2-4 environments per day (out of 5-6 total trained environments; 1-2 for the present study, 4 for classifier training data and another experiment) for 10-15 minutes per environment. Each environment consisted of a square, octagonal, or circular arena (60-70 cm diameter), with shower curtains surrounding the environment and a prominent polarizing visual cue on the environment walls. The environments were at the same physical location but had different colors, patterns, and textures on the walls and floors, as well as different patterns on the shower curtain surrounding the environment. For 18 mice, a single square environment was used for object recording sessions (63 cm x 63 cm, 30 cm high walls; Figure 1C), and objects were present

Please cite this article in press as: GoodSmith et al., Flexible encoding of objects and space in single cells of the dentate gyrus, Current Biology (2022), https://doi.org/10.1016/j.cub.2022.01.023

for all training sessions in this environment. For 3 mice, two square environments were used for object recording sessions (see below). All objects were familiar to the mouse, 4 cm in diameter (at the base), 6 cm tall, and differed in shape, color, and texture. For six mice, a black cylinder and a white rectangular cuboid were used. For all other mice, objects were roughly conical or pyramidal to prevent the top of the object from blocking the recording headstage or tether (Figure 1B).

Once tetrodes reached the DG (determined by the distance the tetrodes had been lowered, local field potential (LFP) patterns, and neuronal activity), object recording days were alternated with days when animals foraged for food in multiple distinct environments (forage recordings). Data from these forage recording days were used to train a classifier to separate between DG cell types (see below). Forage recording days consisted of five 10-15 minute recording sessions. In the first four sessions, mice foraged for food in an open environment, and each of the four sessions was in a different environment. The final session of the day was a repeated exposure to one of the four environments and was not used for any analysis in the present study.

Object recording sessions consisted of alternating standard (STD) sessions, in which two objects were in a standard configuration, and object-manipulation (MAN) sessions. Manipulation sessions included moved-object (MOVE) sessions, in which one of the standard objects was moved to a new location, and added-object (ADD) sessions, in which a third object was added to the environment (Figure 1). Animals foraged for chocolate sprinkles in the environment for 10–15 minutes in each session, and they were removed from the environment between sessions. Each recording day consisted of 2-8 object recording sessions. There was not a fixed number or order of sessions, but different MAN sessions were alternated with STD sessions as long as the mice continued to explore the environments. In total, there were a total of 1513 recording sessions across all recorded putative excitatory cells: 923 STD sessions and 590 MAN sessions (160 ADD and 430 MOVE sessions).

In another set of experiments, DG cells were recorded as mice foraged for food in two square environments. One of the two environments was the same square environment used for all other object recording sessions (Figure 1). A second square environment of the same size, but different cues/features, was also used (Figures 7A and S5B). Object locations within this second environment were identical to the first, and the same set of standard objects was used. On each recording day, mice would first forage for food in one of the environments with objects in the STD configuration (STD_A). Next, one object was moved ($MOVE_A$). This pattern of object manipulation was then repeated in the second environment: A STD session (STD_B) was followed by the same object movement ($MOVE_B$). The recording day ended with one more STD session ($STD1_A$' or STD_B'). All forage and object recording days began and ended with a baseline sleep session, in which mice rested in their home cage for 30+ minutes.

Electrophysiological recordings

A total of 366 well-isolated, putative excitatory cells were recorded from the DG of 18 mice as they foraged for food in an environment that contained discrete objects. An additional 112 cells were recorded on tetrodes in the DG of 3 mice as they foraged for food in two square environments. This number of cells may include some cells recorded across days, although object recordings were typically not performed on consecutive days and tetrodes were lowered slowly each day. Tetrodes were made from 12.5 μm nichrome wires (California Fine Wire) and were electroplated with gold to reduce the impedance to ~200 kOhms. A Digital Lynx SX data acquisition system and Cheetah acquisition software (Neuralynx) were used for recordings. Signals were amplified 1,000–5,000 times and filtered between 600 Hz and 6 kHz (for units) or 1 and 475 Hz (for LFPs). Spike waveforms above a threshold of 40–80 μV were sampled for 1 ms at 32 kHz, and LFPs were continuously sampled at 1 kHz. Tetrodes were lowered to the dentate gyrus over a period of ~2-4 weeks. When tetrodes were near the DG, they were lowered < 30 μm per day. In most mice, if cells were present, brief pulses (≤ 5ms pulses) of blue light were given (following the post-behavior sleep session) to identify adult-born granule cells optogenetically for another experiment. No light pulses were given before behavior on the object recording days analyzed here.

Histological procedures

Mice were deeply anesthetized and perfused with phosphate-buffered saline, followed by 4% paraformaldehyde (PFA). The brain was partially exposed and soaked in PFA for 4 hours before tetrodes were retracted and the brain was removed from the skull and drive. The brain was soaked overnight in PFA then transferred to a 30% sucrose solution until the brain had sunk. The brain was then sliced into 40-50 μm thick coronal sections, mounted, and stained for DAPI (Vector Laboratories). Sections were viewed and photographed using a confocal microscope (Zeiss), and tetrode tracks were identified.

Unit isolation

Single units were isolated offline using custom-written cluster-cutting software (Winclust, J. Knierim). Multiple waveform characteristics, including spike amplitude, peak, and energy, were used to isolate cells. These waveform properties were determined for each tetrode wire and plotted against each other in 2D scatter plots. Waveforms were clustered into units by comparing waveform parameters across all possible wire pairs, and iteratively drawing boundaries in these plots to define clusters that minimized overlap with noise or other clusters. The isolation quality of each unit was rated on a subjective scale from 1 (very good) to 5 (poor), depending on the separation of the cluster from other clusters and background noise. Isolation was judged independent of behavioral firing correlates, and only cells rated as fair or better (categories 1, 2, and 3) were included in the analysis.

Rate maps and place fields

The position of the mouse was monitored by using an overhead camera to track red and green LEDs on the recording headstage. The mouse's position was considered to be the center of these LEDs and corresponded to the location of the animal's head. The image

Please cite this article in press as: GoodSmith et al., Flexible encoding of objects and space in single cells of the dentate gyrus, Current Biology (2022), https://doi.org/10.1016/j.cub.2022.01.023

was divided into a 64 x 48 pixel rate map where each bin/pixel was a ~1.4 x 1.4 cm square. The number of spikes when the animal was in each bin of the map was divided by the amount of time the mouse spent in that bin to determine the average firing rate in each bin. This map was then smoothed using an adaptive binning procedure[96] and spatial information scores were calculated from these rate maps.[96] In rate maps, blue pixels represent a firing rate of zero and red pixels represent the cell's peak firing rate within the session. A p value for the spatial information score was determined by a shuffling procedure in which the spike train and location of the mouse were shifted by a random amount (minimum 30 seconds, with the offset points at the end of the data stream wrapped around to the beginning), and the rate map and spatial information score were recalculated. This procedure was repeated 100 times for each cell, and the number of times that the shuffled spatial information score was higher than the observed value determined the p value for the spatial information score. If the shuffled spatial information score was lower than the observed value for all shuffles, the spatial information score was considered significant ($p < 0.01$).

Cells were considered to have a place field if they had a significant ($p < 0.01$) spatial information score > 0.5 bits/spike, and had a mean firing rate $\geq$ 0.1 Hz and (to exclude putative interneurons) < 10 Hz. For spatially modulated cells, individual place fields were identified by finding all pixels of the rate map where the firing rate of the cell exceeded 20% of the cell's peak firing rate. Any group of 30 or more contiguous pixels that passed this 20% threshold was defined as a place field. The center of a place field (place field centroid) was defined as the center of mass of the pixels in that field, weighted by the firing rate of each pixel.

Any cell with a mean firing rate > 10 Hz during the post-behavior sleep session was excluded from our primary analysis (to exclude putative high-rate interneurons). An additional population of cells had a mean firing rate between 2 and 10 Hz, but no significant spatial firing in any environment. These cells may represent a distinct population of hilar interneurons[37,97] and were also excluded from further analysis. The activity of 75 well-isolated putative interneurons is reported in Figure S1.

QUANTIFICATION AND STATISTICAL ANALYSIS

Cell type classification

Cells were classified as putative granule cells or mossy cells using a random forests classifier.[92,93] Random forests is an ensemble learning method in which a large number of decision tree classifiers are generated using a bootstrapped sample of training data and random subsamples of features. Each classifier receives one vote, and the output with the most votes is the final output of the classifier.

The training data used to generate the classifier was collected on separate recording days. On these days, mice foraged for food in four distinct environments (without objects, Figure 2A). A total of 192 putative excitatory cells from 10 mice recorded in forage sessions (without objects) were used to train the classifier for the present study. Only the first four forage sessions from each day were used (the repeated session was excluded). In similar tasks in rats and mice, most granule cells had no place fields in any environment (and very rarely had place fields in more than one environment) while mossy cells had place fields in all or most environments.[37,38] We therefore could confidently consider cells that did not have place fields in any environment as putative granule cells. Likewise, we considered any cells with place fields in at least three environments as putative mossy cells (Figure 2A). Using this selection criterion, 79 putative granule cells and 62 putative mossy cells were selected. These cells were used as the training data to generate a random forests classifier to separate cell types.

The classifier was trained using firing properties recorded during a post-behavior sleep/rest session (Figure 2B). This recording session consisted of periods of both rest and sleep, and different sleep stages were not separately analyzed. While the spatial firing of cells was used to select putative granule cells or mossy cells for training, no spatial firing features were used for classification. The features used to separate cell types were mean firing rate, burstiness (proportion of interspike intervals that were < 6ms), spike duration (peak to valley of the waveform recorded on the tetrode wire with the largest peak amplitude), and the first principal component of the second derivative of the spike waveform (average waveform of highest amplitude tetrode wire).[38] The random forests classifier consisted of 300 individual decision trees, and three random features were used at each split. As each of the 300 individual decision tree classifiers was created using a bootstrapped sample of the cells in the training data, not every cell was used to generate each decision tree classifier. For each cell in the training data, ~$^1/_3$ of the individual classifiers were trained without using that specific cell. The proportion of cells in the training data that are misclassified by the majority of decision trees that were trained without that cell is the "out-of-bag" error rate and is an estimate of the ensemble classifier's generalization error.[92] The out-of-bag error rate of the present classifier was 5% (Figure S2), suggesting reliable classification between DG cell types. This classifier was applied to the post-behavior sleep data recorded on object recording days to identify cells as putative mossy cells and granule cells. While some cells recorded during object sessions may have also been recorded on a previous forage session day, and thus used as part of the training data, tetrodes were moved ~30 μm daily.

Landmark vector analysis

The method used to define landmark vector cells (LVCs) was modified from a previously described method.[4] For each session, the place field centroids were determined for all place fields in the environment. For sessions with at least two place fields, LVCs were identified using the following procedure. First, vectors connecting each object to each place field centroid were calculated. The difference was then calculated between all pairs of vectors that did not share the same object or the same place field centroid. The pair of such vectors with the smallest difference was determined (see Figure 4A for schematic). Sessions with a minimum vector distance below 7 pixels were attributed to putative LVCs. While a one pixel threshold had been previously used to detect LVCs in the

Please cite this article in press as: GoodSmith et al., Flexible encoding of objects and space in single cells of the dentate gyrus, Current Biology (2022), https://doi.org/10.1016/j.cub.2022.01.023

hippocampus,[4] we used a 7 pixel threshold for two reasons. First, the environment, and thus the size of each pixel, used by Deshmukh and Knierim[41] was larger: the area of 7 pixels in this study roughly equals the area of 1 pixel from Deshmukh and Knierim.[41] Place fields in mice are also less stable than place fields in rats in certain tasks,[98] and there are differences in place field stability between DG and other hippocampal subfields.[53]

The distribution of observed minimum vector differences was compared to a random distribution.[4] To create the random distribution, we first collected all place field centroids from all sessions. Random place field centroids were then assigned to each session. Place field centroids were picked so that the number of randomly assigned place fields equaled the number of recorded place fields in that session, and the distance between all place field centroids was never less than 6 pixels (the minimum distance between place field centroids observed in the data). Vector differences were then calculated for the randomized place field locations (using the same procedure described above) to create the random distribution of minimum vector differences.[4] This analysis results in a randomized distribution with the same number of sessions (and the same number of objects and place fields in each session) as the real data. To determine if the number of LVCs detected in our data exceeded the number expected by chance, we generated 100 separate random distributions using the procedure described above. For each of these 100 random distributions, the number of sessions with a minimum vector difference $\leq$ 7 pixels (detected LVCs) was determined. The proportion of random distributions where the number of detected LVCs exceeded the number of LVCs observed in the real data was considered to be the p value for this comparison. To determine whether our selection of 7 pixels for the LVC detection threshold affected these results, the shuffling procedure was repeated with a 5 pixel threshold (Figure S3A), and with a series of threshold values ranging from 1 to 20 pixels (Figure S3B).

Distance to nearest place field

We first identified each MAN session and its preceding STD session and analyzed all pairs of sessions in which at least one place field was present in both sessions. While multiple session pairs could come from the same cell, different session pairs reflect distinct object manipulations (no object manipulations were repeated on the same day). The location of the manipulated object (new object or moved object) in the MAN session was determined ("X" in Figure 6A, top). The distance from this location to the nearest place field centroid was determined in both the STD and MAN sessions, and the difference between these minimum distances was determined. If a field was near the object location in the MAN session but not in the STD session (e.g., fields appearing at that location or fields moving with the moved object), this difference value would be high, indicating that the place field location was influenced by object manipulation.

As some amount of place field drift and remapping is expected, we repeated the same analysis at the location of the unmanipulated object (Figure 6A). If there was significant remapping or place field drift unrelated to object manipulations, a similar distribution of difference values would be expected at that location. However, if the reduction in distance between the object location and the nearest place field exceeded the 95th percentile of the values obtained using the unmanipulated object location, the reduction was considered to be significant.

Rate map correlation analysis

For overall rate map correlation comparisons, all sets of three consecutive sessions that consisted of two STD sessions with a MAN (MOVE or ADD) session between them (STD1 – MAN – STD2) were identified (see Figure 6C for schematic). Only groups of sessions with at least one place field in at least one of the three sessions were analyzed. Rate map correlations were calculated between the rate maps for the STD1 and STD2 sessions (R_{STD}) and the STD1 and MAN sessions (R_{MAN}). The difference between R_{STD} and R_{MAN} was then calculated and compared to a shuffled distribution (Figure 6C), in which the STD1 map in each group of sessions was replaced with another random STD1 map from another spatially-modulated cell, and the analysis was repeated. This process was repeated 1000 times to generate a shuffled distribution of correlation differences. Cells with correlation difference values that exceeded the 95th percentile of the shuffled distribution were considered to be significant.

"Local rate map" correlations were calculated by first identifying all STD sessions followed by a MOVE session. For each session pair, one object was moved in the MOVE session, and the other object was in the same location in the STD and MOVE sessions. The locations of all objects in the STD and MOVE sessions were determined, and "local rate maps" were created for all object locations in both sessions (STD object locations in STD and MOVE sessions, and MOVE object locations in STD and MOVE sessions). Each local rate map was centered at an object location and consisted of ± 10 pixels in each direction from the object, generating a 21x21 pixel local rate map. The STD rate maps were thresholded to only include activity within place fields (any pixels with a rate < 20% of the peak firing rate were set to 0). The "spatial" rate map correlation was calculated between maps centered at the same spatial location in the STD and MOVE session (the location of the moved object in the MOVE session), and the "object-related" rate map correlation was calculated between maps centered at the location of the moved object in both the STD and MOVE session (Figure 6E). The difference between the "spatial" and "object-related" correlations was calculated. This distribution was compared to the distribution generated by repeating the analysis centered at the location of the unmoved object in each MOVE session. For the "unmoved" object correlations, the "spatial" correlation was calculated as the correlation between maps centered at the location of the unmoved object in both STD and MOVE sessions, and the "object-related" correlation was calculated as the correlation between maps centered at the unmoved object location in the STD session, and the moved object's new location in the MOVE session (as if the unmoved object were the object that was moved) (Figure 6E). Cells were considered to have a significantly higher "object-related" than "spatial" correlation if the difference between these values exceeded the 95th percentile of the distribution from the "unmoved" object.

Please cite this article in press as: GoodSmith et al., Flexible encoding of objects and space in single cells of the dentate gyrus, Current Biology (2022), https://doi.org/10.1016/j.cub.2022.01.023

Subjective response type evaluation

To assign putative object responses to individual cells and compare these responses between different environments, we subjectively evaluated object recording sessions. For all cells with place fields, each MOVE session and its preceding STD session were evaluated separately. Only pairs of sessions in which at least one place field was detected in at least one of the two sessions were evaluated. Putative object responses were then assigned to these session pairs.

Three observers (D.G., S.H.K., and K.M.C) separately evaluated the session pairs for object-related responses. Each of the session pairs with at least one place field in at least one session was presented in random order. For each session pair (STD and MOVE), the rate maps, object locations, and firing rates for that pair of sessions was displayed. No other information about the cell or its activity in other recording sessions was presented. The observer would then make a judgment on how object movement had affected the cell's activity. Cells were classified as 1) no object response/stable spatial firing, 2) Moved and/or rotated field, 3) Appear, 4) Disappear, 5) Trace, or 6) Capture (see Figure 5 for examples of each response type). If multiple clear responses could be detected, each response was recorded. Each observer repeated their evaluation of the session pairs three times (different random order each time), and the response type assigned to the session pair at least 2/3 times was considered their assessment for that session pair. On average, individual observers picked the same response at least two of the three times for 99.6% of session pairs (range 99% - 100%), and the same response was selected all three times for 78% of session pairs (range 75% - 82%).

The subjective response assignments from each observer were then compared. The response assigned by at least two of the three observers was considered the response of that pair of sessions. For 87 of the 95 session pairs (92%), two of the three observers selected the same response type. Session pairs where no two observers selected the same response category were considered ambiguous responses (8 session pairs, 8%).

The probability of observing any specific object-related change in activity was determined across the entire population of session pairs (in both environments). This probability was used to calculate joint probabilities and estimate how much overlap of object-related activity between environments would be expected by chance.

Statistical tests

Statistical tests were calculated in Matlab. Data represent median and interquartile range (IQR). The p values of Wilcoxon rank-sum tests, Wilcoxon signed-rank tests, and χ^2 tests represent the results of two-tailed tests, and results were considered significant if the p value was < 0.05. A χ^2 goodness-of-fit test was used to compare the proportion of cells with object-related activity changes in multiple environments to expected values. The expected values of object-related activity in multiple environments were calculated from the joint probability of detected object-related responses. When comparing observed data to a shuffled or random distribution, cells that passed the 95th percentile of the shuffled or random distribution were considered to be significant at $p < 0.05$. The proportion of cells that exceeded the 95th percentile was then compared to the null hypothesis that 5% of values would exceed the 95th percentile using a one proportion z-test (test for proportions); p values for the test for proportions are results of one-tailed tests.